



Braincase anatomy of the early sauropodomorph *Saturnalia tupiniquim* (Late Triassic, Brazil)

Mario Bronzati, Max C. Langer & Oliver W. M. Rauhut

To cite this article: Mario Bronzati, Max C. Langer & Oliver W. M. Rauhut (2019): Braincase anatomy of the early sauropodomorph *Saturnalia tupiniquim* (Late Triassic, Brazil), *Journal of Vertebrate Paleontology*

To link to this article: <https://doi.org/10.1080/02724634.2018.1559173>

 View supplementary material 

 Published online: 19 Mar 2019.

 Submit your article to this journal 

 View Crossmark data 

BRAINCASE ANATOMY OF THE EARLY SAUROPODOMORPH *SATURNALIA TUPINIQUIM* (LATE TRIASSIC, BRAZIL)

MARIO BRONZATI, *^{1,2,3} MAX C. LANGER, ¹ and OLIVER W. M. RAUHUT ^{2,3}

¹Laboratório de Paleontologia, Faculdade de Filosofia, Ciências e Letras de Ribeirão Preto, Universidade de São Paulo, Ribeirão Preto, São Paulo, 14040-901, Brazil,

mariobronzati@gmail.com; mclanger@ffclrp.usp.br;

²Bayerische Staatssammlung für Paläontologie und Geologie, Munich, 80333, Germany, o.rauhut@lrz.uni-muenchen.de;

³Faculty of Geosciences, Ludwig Maximilians University of Munich, Munich, 80333, Germany

ABSTRACT—The braincase anatomy of the sauropodomorph dinosaur *Saturnalia tupiniquim* from the Upper Triassic (Carnian) Santa Maria Formation of Brazil is described for the first time using computed tomography (CT). The braincase is characterized by a semilunar depression on the lateral surface of the basisphenoid, an occipital condyle whose ventral margin lies dorsal to the ventral margin of the cultriform process of the parabasisphenoid, a poorly developed preotic pendant, and anteriorly oriented basiptyergoid processes. The comparative description improves our understanding of the early dinosaur braincase, which is poorly known relative to that of later representatives of the group. In addition, we discuss braincase features recently employed to investigate the phylogenetic relationships of dinosauromorphs, especially the pneumatic recesses of the braincase. Our study indicates that the semilunar depression and basioccipital recess are more widespread among dinosaurs and their closest archosauriform relatives than previously suggested. These structures are present in the three main dinosaurian lineages and also in non-dinosaurian dinosauromorphs, indicating that they might be plesiomorphic for Dinosauria. Likewise, the subsellar and basisphenoid recesses were observed in all examined dinosauromorph taxa, with variation observed in the relative development of these structures but not in their presence/absence. Our character reassessments and discussion of morphological variation as parts of transformation series strengthen the basis for integrating braincase features in future studies of dinosauromorph phylogeny.

SUPPLEMENTAL DATA—Supplemental materials are available for this article for free at www.tandfonline.com/UJVP. The underlying research materials for this article can be accessed in the MorphoSource Repository at: http://www.morphosource.org/Detail/ProjectDetail/Show/project_id/553.

Citation for this article: Bronzati, M., M. C. Langer, and O. W. M. Rauhut. 2019. Braincase anatomy of the early sauropodomorph *Saturnalia tupiniquim* (Late Triassic, Brazil). *Journal of Vertebrate Paleontology*. DOI: 10.1080/02724634.2018.1559173.

INTRODUCTION

Braincase anatomy of dinosaurs has been investigated in some detail. Most of these works, however, focus on Jurassic and Cretaceous taxa (e.g., Janensch, 1935; Galton, 1985; Currie, 1997; Tykoski, 1998; Currie and Zhao, 2004; Rauhut, 2004; Sampson and Witmer, 2007; Knoll et al., 2012; Sobral et al., 2012; Paulina-Carabajal et al., 2014), with detailed studies of Late Triassic dinosaurs (e.g., Galton, 1984, 1985; Galton and Bakker, 1985; Martínez et al., 2012b; Apaldetti et al., 2014; Bronzati and Rauhut, 2017; Müller et al., 2018) and non-dinosaurian dinosauromorphs (Bittencourt et al., 2014) being relatively scarce. It thus seems safe to conclude that our understanding of the anatomy and evolution of the early dinosaur braincase lags behind the other parts of their skeleton (Langer, 2003; Langer et al., 2007; Butler, 2010; Sereno et al., 2012).

Various factors contribute to this relatively poor state-of-knowledge. The braincase is not preserved in many Triassic taxa (*Chromogisaurus novasi*, *Staurikosaurus pricei*, *Guaibasaurus candelariensis*, *Chindesaurus briansmalli*, *Pisanosaurus mertii*, *Pampadromaeus barbarenaei*), whereas in other forms it

is incomplete/fragmentary (*Eocursor parvus*, *Eodromaeus murphi*) or partially obscured due to the articulated nature of the skull (*Herrerasaurus ischigualastensis*, *Eoraptor lunensis*). In addition, the complete or nearly complete braincase of some critical taxa, such as *Tawa hallae* and *Saturnalia tupiniquim*, still awaits detailed description.

Here, we describe the braincase anatomy of *Saturnalia tupiniquim*, from the Upper Triassic (Carnian, ca. 230 Ma) of Brazil. *Saturnalia tupiniquim* was first described by Langer et al. (1999) and is consistently recovered as a sauropodomorph in phylogenetic analyses (Nesbitt et al., 2009, 2010; Ezcurra, 2010; Martínez et al., 2011, 2012a; Cabreira et al., 2016; Baron et al., 2017). The postcranial, particularly the appendicular, anatomy of *S. tupiniquim* is well documented (Langer, 2003; Langer et al., 2007), but its braincase has never been described in detail. Given its age and phylogenetic position, *S. tupiniquim* is likely a key taxon for studies aimed at the origin and early evolution of Dinosauria and Sauropodomorpha. Because the braincase of non-sauropodan sauropodomorphs has been discussed recently (Fedak and Galton, 2007; Martínez et al., 2012b; Bronzati and Rauhut, 2017; Bronzati et al. 2018; Chapelle and Choiniere, 2018), this study will focus on braincase anatomy and evolution in early dinosaurs and non-dinosaurian dinosauromorphs.

Institutional Abbreviations—AMNH, American Museum of Natural History, New York, U.S.A.; BPI, Evolutionary Studies Institute (formerly Bernard Price Institute for Palaeontological

*Corresponding author.

Color versions of one or more of the figures in the article can be found online at www.tandfonline.com/ujvp.

Research), University of the Witwatersrand, Johannesburg, South Africa; **CAPPA/UFSM**, Centro de Apoio à Pesquisa Paleontológica, da Quarta Colônia/Universidade Federal de Santa Maria, Santa Maria, Brazil; **GR**, Ghost Ranch Ruth Hall Museum of Palaeontology, Abiquiu, New Mexico, U.S.A.; **MB**, Museum für Naturkunde, Berlin, Germany; **MCP**, Museu de Ciências e Tecnologia, Pontifícia Universidade Católica do Rio Grande do Sul, Porto Alegre, Brazil; **NHMUK**, Museum of Natural History, London, U.K.; **OUMNH**, Oxford University Museum of Natural History, Oxford, U.K.; **PVL**, Paleontología de Vertebrados Lillo, Tucuman, Argentina; **PVSJ**, Museo de Ciencias Naturales, San Juan, Argentina; **PULR**, Universidad Nacional de La Rioja, La Rioja, Argentina; **QG**, Queen Victoria Museum, Salisbury, Zimbabwe; **SAM**, Iziko South African Museum, Cape Town, South Africa; **SMNS**, Staatliches Museum für Naturkunde, Stuttgart, Germany; **UFSM**, Universidade Federal de Santa Maria, Santa Maria, Brazil; **ULBRA-PV**, Museu de Ciências Naturais, Universidade Luterana do Brasil, Canoas, Brazil; **ZPAL**, Institute of Paleobiology of the Polish Academy of Sciences, Warsaw, Poland.

MATERIALS AND METHODS

The Braincase of *Saturnalia tupiniquim*

Saturnalia tupiniquim is known based on three fairly complete specimens: MCP 3844-PV (holotype) and MCP 3845-PV and 3846-PV (paratypes); see Langer (2003) for more details. A preliminary description (Langer et al., 1999) was followed by more detailed accounts of specific skeletal areas: pelvic girdle and hind limb (Langer, 2003) and shoulder girdle and forelimb (Langer et al., 2007). The braincase is only preserved in MCP 3845-PV. An account of the endocranial and inner-ear cavities was presented elsewhere (Bronzati et al., 2017), but the details of braincase osteology remain undescribed.

CT Scan

The block containing the specimen (Fig. 1) is heavily fractured, making mechanical preparation risky; hence, we employed

computed tomography (CT) scanning. The specimen was scanned at the Zoologische Staatssammlung München (Bavaria State Collection of Zoology, Munich, Germany) in a Nanotom Scan (GE Sensing and Inspection Technologies, Wunstorf, Germany) using the following parameters: voltage, 100 kV; current, 130 μ A; and 3.1 μ m voxel size. A total of 1,440 X-ray slices were generated; these were down-sampled by half and then segmented in Amira (version 5.3.3; Visage Imaging, Berlin, Germany).

DESCRIPTION

Comparative taxa and the source of information (first-hand analysis and/or the literature) are detailed in Table 1. Reference to collection numbers and/or previous studies are provided in the description only if they differ from those in Table 1.

General Aspects of the Braincase

The preserved braincase includes the parabasisphenoid, basioccipital, supraoccipital, prootics, otoccipitals (= exoccipital + opisthotic sensu Sampson and Witmer, 2007), and laterosphenoids. Not all bone sutures are visible, probably due to a combination of advanced fusion and tomographic artifacts. For instance, the otoccipital-basioccipital suture at the dorsolateral portion of the occipital condyle is clearly visible with the naked eye here and in other examined dinosauriforms. Nevertheless, this suture is not recognizable in the CT data of *Saturnalia tupiniquim*. It is important to point out this situation because it hampers a more detailed description of those elements preserved inside the matrix. Nevertheless, most braincase structures (e.g., cranial nerve foramina, recesses) are identified and described in detail below.

The laterosphenoids are isolated elements, whereas the supraoccipital, otoccipitals, parabasisphenoid, basioccipital, and

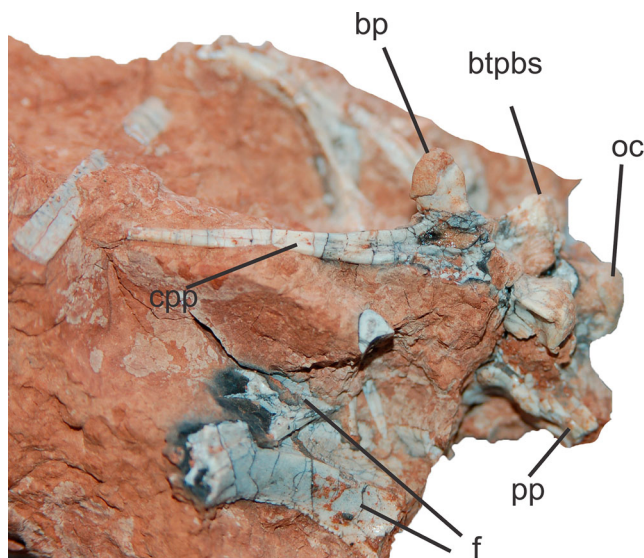


FIGURE 1. General view of the block containing the braincase of the specimen MCP 3845-PV of *Saturnalia tupiniquim*. **Abbreviations:** bp, basipterygoid process; **btpbs**, basisphenoid component of the basal tubera; **cpp**, cultriform process of the parabasisphenoid; **f**, frontal; **oc**, occipital condyle; **pp**, paroccipital process.

TABLE 1. List of comparative taxa used in the present study.

Taxon	Source of information
<i>Adeopapposaurus mognai</i>	PVSJ 568; PVSJ 610
<i>Buriolestes schultzi</i>	CAPPA/UFSM 0035
<i>Coloradisaurus brevis</i>	PVL 3967
<i>Eocursor parvus</i>	SAM-PK-K8025
<i>Eodromaeus murphi</i>	PVSJ 562
<i>Eoraptor lunensis</i>	PVSJ 512
<i>Euparkeria capensis</i>	SAM-PK-7696; SAM-PK-5867
<i>Herrerasaurus</i>	PVSJ 407
<i>ischigulastensis</i>	
<i>Hypsilophodon foxii</i>	OUMNH R2477
<i>Ixalerpeton polesinensis</i>	ULBRA-PVT059
<i>Lesothosaurus</i>	NHMUK PV R8501
<i>diagnosticus</i>	
<i>Lewisuchus admixtus</i>	PULR 01
<i>Marasuchus lilloensis</i>	PVL 3872
<i>Massospondylus carinatus</i>	SAM-PK-K1314
<i>Megapnosaurus</i>	QG 195; QG 197
<i>rhodesiensis</i>	
<i>Pantyrdraco caducus</i>	NHMUK-P.24; NHMUK-P.141/1
<i>Plateosaurus engelhardti</i>	MB.R.5586-1; SMNS 13200; Prieto-Marquez and Norell, 2011
<i>Prolacerta broomi</i>	BP/1/5066
<i>Silesaurus opolensis</i>	ZPAL Ab III/361; ZPAL Ab III/362
<i>Sphenosuchus acutus</i>	SAM-PK-K3014
<i>Tawa hallae</i>	GR 241
<i>Thecodontosaurus</i>	Benton et al., 2000
<i>antiquus</i>	
<i>Unaysaurus toletinoi</i>	UFSM 11069

Collection numbers designate specimens analyzed first hand by the authors, whereas other comparative data were obtained from the literature listed within the table.

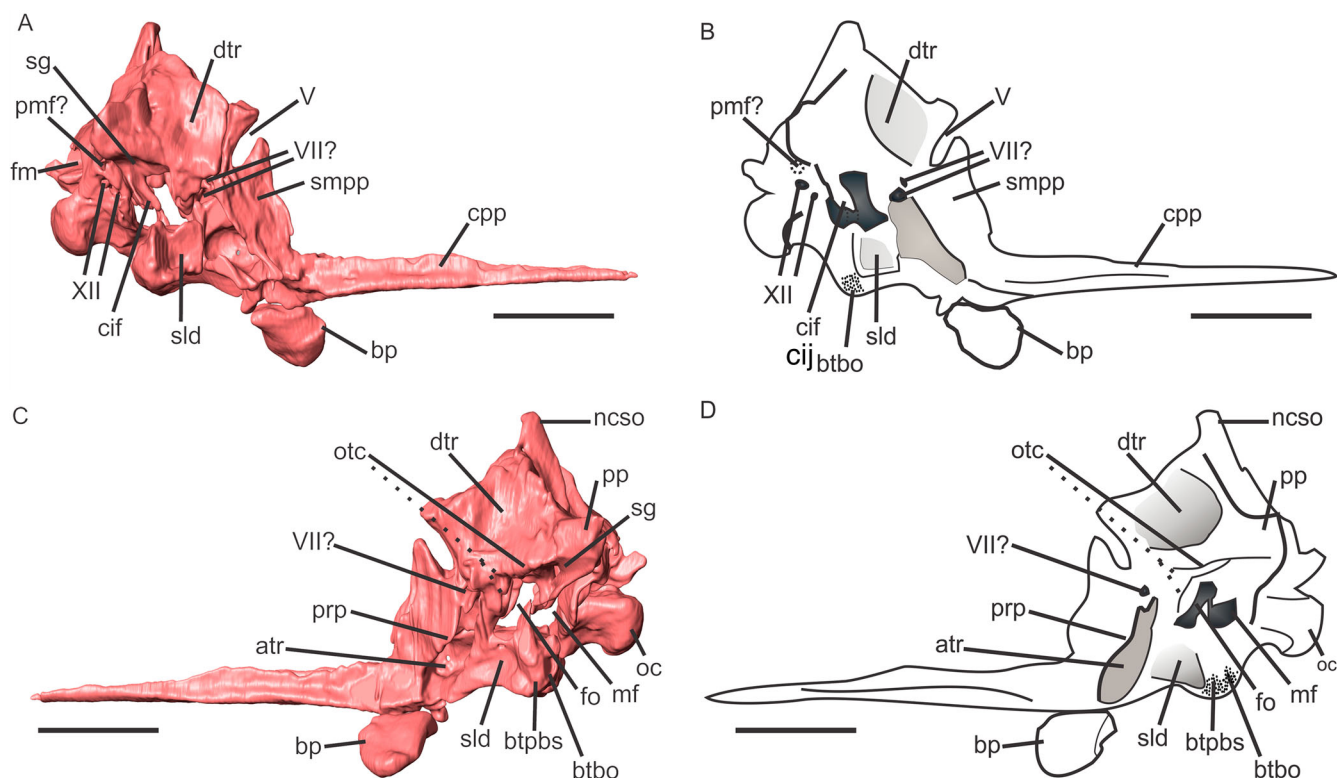


FIGURE 2. Three-dimensional reconstruction of the braincase of the specimen MCP 3845-PV of *Saturnalia tupiniquim* in right (A, B) and left (C, D) lateral views. **Abbreviations:** atr, anterior tympanic recess; bp, basiptyergoid process; btbo, basioccipital component of the basal tubera; btpbs, basisphenoid component of the basal tubera; cif, crista interfenestralis; cpp, cultriform process of the parabasisphenoid; dtr, dorsal tympanic recess; fm, foramen magnum; fo, fenestra ovalis; mf, metotic foramen; ncsso, nuchal crest of the supraoccipital; oc, occipital condyle; otc, otosphenoidal crest; pmf, additional foramen posterior to the metotic foramen; pp, paroccipital process; prp, preotic pendant; sg, stapedia groove; sld, semilunar depression; smpp, surface for attachment of the protractor pterygoideus muscle (including the preotic pendant); VII, foramen for the facial nerve; XII, foramen for the hypoglossal nerve. Scale bars equal 1 cm.

prootics are preserved in articulation (Fig. 2). A break separated parts of the basioccipital and otoccipital, including the occipital condyle, from the other elements. These were glued in place before CT scanning. A second line of fracture is visible in the CT data running horizontally through the region occupied by the fenestra ovalis and metotic foramen (Fig. 2). This fracture likely does not follow the natural junctions between the dorsal (prootic, otoccipitals, supraoccipital) and ventral (basioccipital and parabasisphenoid) components of the braincase but rather marks a plane structurally weakened by these large lateral openings (which also include the openings for the trigeminal [CN V] and facial [CN VII] nerves). This preservational pattern is also seen in two braincases of the sauropodomorph *Platiosaurus* (MB.R.5855.1 and AMNH 6810). Regarding MCP 3845-PV, the portion of the otoccipitals containing the hypoglossal canals (CN XII) is thus preserved in articulation with the ventral piece of the braincase that includes the basioccipital and parabasisphenoid. The larger portion of the otoccipitals is articulated to the dorsal braincase elements, including the prootic and supraoccipital.

Specimen MCP 3845-PV compares closely in size with the holotype but is more gracile; this prompted Langer et al. (2007) to argue that MCP 3845-PV is a juvenile or subadult that had reached near adult size. Regarding the braincase, sauropodomorph specimens considered juvenile (based on their cranial and postcranial anatomy), such as *Efraasia minor* (Galton and Bakker, 1985), *Pantydraco caducus* (Galton and Kermack, 2010), *Anchisaurus polizelus* (Fedak and Galton, 2007), and *Unaysaurus toletinoi* (J. Bittencourt, pers. comm.), retain an

open basioccipital-parabasisphenoid contact, with these elements preserved disarticulated (Bronzati and Rauhut, 2017). Outside Sauropodomorpha, the lack of closed braincase sutures in the holotype of *Tawa hallae* was used to argue its juvenile status (Nesbitt et al., 2009). In this context, the well-developed articulation between the basioccipital and the parabasisphenoid of MCP 3845-PV suggests that the specimen is skeletally mature and therefore not a juvenile. On the other hand, the frontals are disarticulated (Fig. 1); a late subadult stage (Langer et al., 2007) seems most plausible. However, assessing maturity in an individual based solely on the patterns of sutural closure might be misleading (Bailleul et al., 2016).

The anteroposterior length of the braincase, from the occipital condyle to the tip of the cultriform process, is 54 mm, approximately half the total estimated skull length of 100 mm (Langer et al., 1999). This ratio cannot be established precisely for most early dinosaurs, either because the anterior tip of the cultriform process is hidden by matrix or other bones (e.g., *Eoraptor lunensis*, *Herrerasaurus ischigualastensis*) or simply because the material is incomplete (e.g., *Panphagia protos*, *Pantydraco caducus*). Nevertheless, the ratio in *Saturnalia tupiniquim* roughly approaches that of the sauropodomorph *Massospondylus carinatus* (0.5 in BPI 5241; and ca. 0.6 in SAM-PK-K1314) and the ornithischian *Lesothosaurus diagnosticus* (ca. 0.5). The latter, however, lacks the anterior tip of the premaxilla, so that total skull length cannot be established precisely.

Basioccipital—The basioccipital is the most completely exposed bone in the braincase block, and some of its limits are also more easily recognizable in the CT data (Figs. 2–4). It

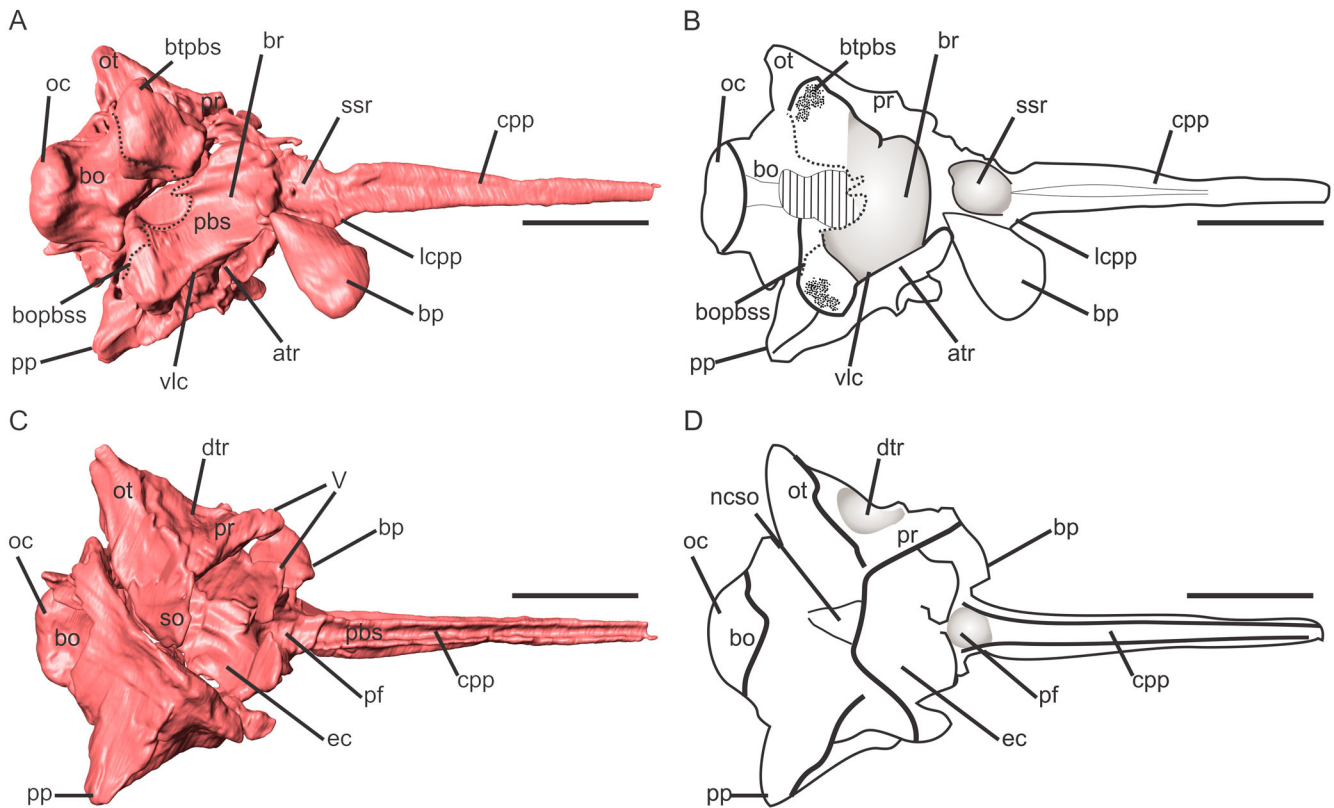


FIGURE 3. Three-dimensional reconstruction of the braincase of the specimen MCP 3845-PV of *Saturnalia tupiniquim* in ventral (A, B) and dorsal (C, D) views. **Abbreviations:** atr, anterior tympanic recess; bo, basioccipital; bopbss, basioccipital-parabasisphenoid suture (dashed line); bp, basipterygoid process; br, basisphenoid recess; btbo, basioccipital component of the basal tubera; btpbs, basisphenoid component of the basal tubera; cpp, cultriform process of the parabasisphenoid; dtr, dorsal tympanic recess; ec, endocranial cavity; lcpp, lamina of the cultriform process of the parabasisphenoid; ncsso, nuchal crest of the supraoccipital; oc, occipital condyle; ot, otoccipital; pbs, parabasisphenoid; pf, pituitary fossa; pp, paroccipital process; pr, prootic; so, supraoccipital; ssr, subsellar recess; vlc, ventrolateral crest; V, notch for the trigeminal nerve. Scale bars equal 1 cm.

forms the posteroventral portion of the basicranium, contacting the parabasisphenoid anteriorly and the otoccipitals dorsally. The bone is preserved in two separate pieces, a posterior piece including the occipital condyle and an anterior piece attached to the parabasisphenoid (Fig. 3). The former was glued to the anterior portion of the braincase before scanning. The basioccipital is almost complete, missing only a small part of its ventral surface between the posterolateral projections of the parabasisphenoid and a part of the surface that would have contacted the otoccipital on the left side, anterior to the occipital condyle (Figs. 1–3). In general, the bone is composed of an anterior portion, corresponding to an anterior projection extending between the posterolateral projections of the parabasisphenoid, and a posterior portion including the occipital condyle (Figs. 1–4).

The basioccipital-parabasisphenoid contact is ‘U’/‘V’-shaped, with an anterior projection of the former extending between two posterolateral expansions of the latter (Fig. 3). This is the expected morphology for non-sauropodan sauropodomorphs (Bronzati and Rauhut, 2017) and is also observed in the silesaurid *Silesaurus opolensis* (Piechowski et al., 2018:fig. 5B), the sauropsid *Tawa hallae*, and the ornithischians *Dysalotosaurus lettowvorbecki*, *Lesothosaurus diagnosticus*, and *Eocursor parvus*. The basioccipital and basisphenoid are not articulated in *T. hallae* and *E. parvus*, but an excavation on the posterior surface of their parabasisphenoid is compatible with a ‘U’/‘V’-shaped contact. The anterior projection of the basioccipital corresponds to slightly less than half the total anteroposterior length of the

bone, which is 11 mm (Fig. 2). The lateromedial width of the projection at its posterior third is also 5 mm, and this subtly diminishes anteriorly, ending in a rounded margin and giving a ‘U’ shape to this portion of the bone (Fig. 3). The CT data show that the ventral surface of that projection is transversely concave, confluent with, and deeper than, the basisphenoid recess. However, this region is damaged and mostly covered by matrix, hampering a more precise reconstruction.

The posterior portion of the basioccipital (Fig. 3) is narrower at the occipital condyle (width = 6 mm) than at the basioccipital basal tubera (width = 9.5 mm). Its ventral surface is anteroposteriorly concave, and as smooth as in *Lewisuchus admixtus*, *Silesaurus opolensis*, and *Adeopapposaurus mognai*. These taxa lack the parallel ridges extending from the occipital condyle to the basal tubera described for *Efraasia minor* (Bronzati and Rauhut, 2017) and also seen in *Plateosaurus engelhardti* and *Tawa hallae*. In *T. hallae*, these ridges define the subcondylar recess medially (see below), a depression in the ventral surface of the basioccipital anterolateral to the occipital condyle (Witmer, 1997).

In cross-section, the posterior portion of the basioccipital (anterior to the occipital condyle) has ventrolaterally facing surfaces that form an angle of approximately 120° to one another. This ‘U’-shaped morphology, together with the lack of the paired ridges mentioned above, blurs the distinction between ventral and lateral surfaces. Nevertheless, a fossa is seen in both anterolateral corners of this basioccipital portion (Fig. 3); these correspond topologically to the subcondylar recess of

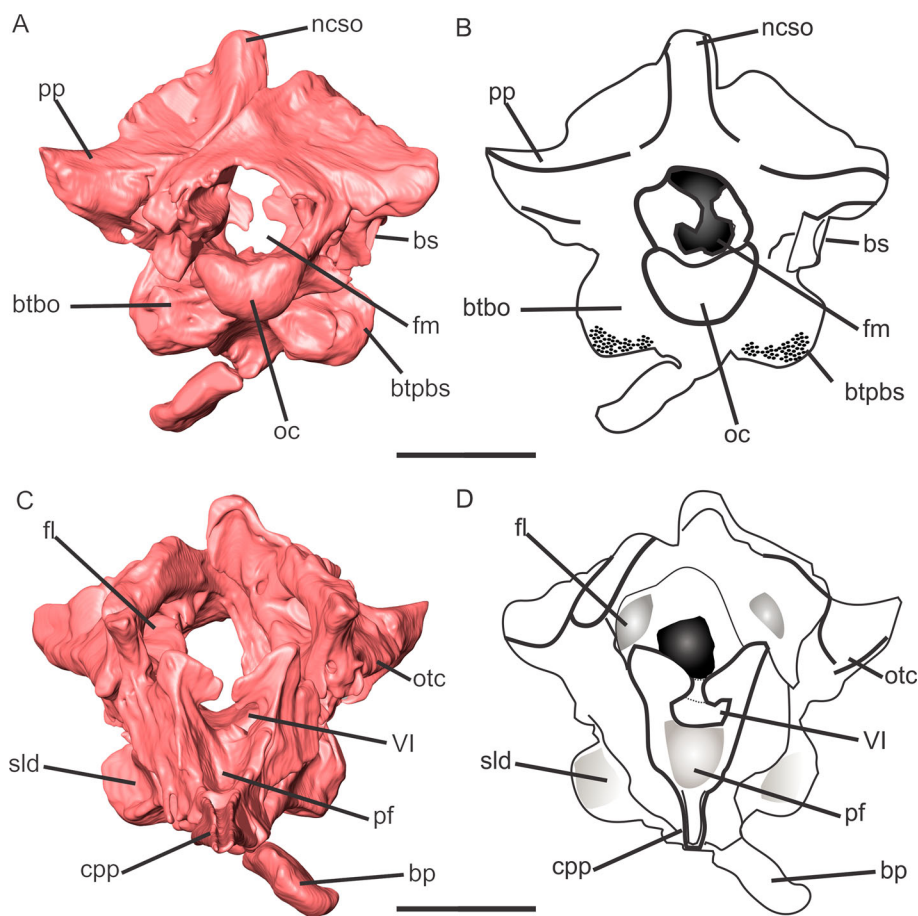


FIGURE 4. Three-dimensional reconstruction of the braincase of the specimen MCP 3845-PV of *Saturnalia tupiniquim* in posterior (A, B) and anterior (C, D) views. **Abbreviations:** **bp**, basipterygoid process; **bs**, bony strut; **btbo**, basioccipital component of the basal tuber; **btpbs**, basisphenoid component of the basal tuber; **cpp**, cultriform process of the parabasisphenoid; **fl**, flocular recess; **fm**, foramen magnum; **ncso**, supraoccipital nuchal crest; **oc**, occipital condyle; **otc**, otosphenoidal crest; **pf**, pituitary fossa; **pp**, paroccipital process; **sld**, semilunar depression; **VI**, notch for the abducens nerve. Scale bars equal 1 cm.

neotheropods (sensu Witmer, 1997). Albeit with a certain degree of subjectivity, the fossa of *Saturnalia tupiniquim* is not as well developed as that of *Tawa hallae* or *Buriolestes schultzi* but more closely resembles those of *Efraasia minor* and *Plateosaurus engelhardti*.

The occipital condyle is kidney-shaped (concave dorsally) in occipital view (Fig. 4). As for all dinosauriforms (Sampson and Witmer, 2007; Bittencourt et al., 2014; Bronzati and Rauhut, 2017), the occipital condyle is mostly composed of the basioccipital, with a small otoccipital contribution to its dorsolateral corners. The condyle is 8 mm wide, half of which corresponds to the basioccipital, and the other half to the otoccipital (2 mm on each side). Its midline height is 4 mm. This remains relatively constant along the lateromedial extension of the structure, because its dorsal and ventral surfaces are concave and convex, respectively.

The maximum width of the foramen magnum is 95 mm, reached at mid-length of its dorsoventral axis (Figs. 3, 4). The foramen magnum is wider than tall, as in *Lewisuchus admixtus*, with a maximum height of 55 mm. In *Silesaurus opolensis*, *Herrerasaurus ischigualastensis*, and *Plateosaurus engelhardti*, the foramen magnum is approximately as wide as tall. The foramen magnum of dinosaurs is typically surrounded by the basioccipital medioventrally, the supraoccipital mediodorsally, and the otoccipital laterodorsally, with their relative contributions varying between taxa (Sampson and Witmer, 2007; Bronzati and Rauhut, 2017). In MCP 3845-PV, only the basioccipital contribution can be precisely defined.

The dorsal surface of the basioccipital (accessible with CT; see Fig. S1) forms most of the endocranial floor in the posterior half of the braincase. The only exception is a small contribution of the otoccipitals to its lateral portion, at the level of the occipital condyle. The dorsal surface of the basioccipital is transversely concave, forming a ‘U’-shaped endocranial floor in this region. The floor of the endocranial cavity is slightly narrower posteriorly, at the anterior limit of the occipital condyle, than anteriorly, where the anterodorsal portion of the basioccipital forms the ventral border of the metotic foramen.

Parabasisphenoid—In dinosauriforms (Bittencourt et al., 2014), including dinosaurs (Sampson and Witmer, 2007), the parasphenoid and basisphenoid are usually fused, forming the parabasisphenoid (sensu Gower and Weber, 1998). In MCP 3845-PV, the parabasisphenoid contacts the prootics anterodorsally, the otoccipitals posterodorsally, and the basioccipital posteriorly (Figs. 2, 3). It forms the anterior part of the basicranium, and also a large portion of its lateral walls, cultriform and basipterygoid processes, basisphenoid component of the basal tubera, and preotic pendant (see prootic description below). The parabasisphenoid also contributes to the subsellar, basisphenoid, otic, and anterior tympanic recesses.

The cultriform process is here considered the portion of the parabasisphenoid extending anteriorly from the subsellar recess, between the basipterygoid processes (Fig. 3). In MCP 3845-PV, the process is 30 mm long, corresponding to ca. 55% of the total anteroposterior length of the braincase. The process is

4 mm broad at its posterior end and gradually narrows anteriorly, with a distal width of 1.5 mm. The height of the process also decreases anteriorly; it is 5.3 mm proximally and no more than 2 mm distally. In cross-section, the anterior third of the cultriform process is ‘U’-shaped, with a rounded ventral margin. Posteriorly, the cross-section assumes the shape of an inverted ‘T,’ with the presence of short (1 mm), bulbous lateral projections that are the cross-sectional expression of ridges extending along the ventral surface of the bone. These parallel ridges extend for about half the length of the cultriform process, becoming lower anteriorly. Anterior to that, the ventral surface of the process flattens. Posteriorly, the ridges merge with the base of the basiptyergoid processes (Fig. 3), forming the lamina of the cultriform process of the parabasisphenoid (Bronzati and Rauhut, 2017), i.e., the triangular lateral lamina of the parabasisphenoid rostrum of Apaldetti et al. (2014). Medial to these laminae, a recess at the anterior portion of the main body of the parabasisphenoid is identified as the subsellar recess (Fig. 3). Its borders are preserved only on the left side of the braincase (covered by matrix but visible with the CT data). The right side of this region is severely damaged. The recess is 5 mm wide and 5 mm deep. Although its anterior margin is not entirely preserved, the recess likely had a subcircular outline in ventral view.

The ventral surface of the parabasisphenoid, excluding the cultriform process, would assume an ‘X’ shape with both basiptyergoid processes preserved (Fig. 3), the basiptyergoid processes corresponding to the anterolateral projections, with the posterolateral projections formed by the basisphenoidal component of the basal tubera (Fig. 3). As such, the parabasisphenoid body has a total anteroposterior length of 12 mm. Immediately posterior to the subsellar recess, the parabasisphenoid is 7 mm wide but expands posteriorly, being 19 mm wide at the basal tubera. It is worth mentioning that this width includes the ‘gap’ in the parabasisphenoid that receives the anterior projection of the basioccipital. The ventral edge of the posterior margin of the bone is dorsally located in relation to the ventral extension of its main body, so that a curved posteroventral margin is formed in lateral view.

Each posterior projection of the parabasisphenoid is 6 mm long (Fig. 3). Each contribution to the basal tubera is a bulbous structure, with an uneven surface covered in small and shallow pits reflecting muscle attachment. The pits are concentrated in the posterior and ventral surfaces of the tuber, but they also cover the ventral portion of the lateral surface of the parabasisphenoid in this area.

The depression on the ventral surface of the main body of the parabasisphenoid (Fig. 3), located posterior to the subsellar recess, is here identified as the basisphenoid recess (sensu Witmer, 1997; see Discussion, below). A thin and low wall forms the anterior limit of the depression, marking its separation from the subsellar recess. Laterally, the basisphenoid recess is bounded by the ventrolateral crest (sensu Kurzanov, 1976; = lateral lamina of the basisphenoid of Apaldetti et al., 2014). The crest is laminar, marking the boundary between the ventral and lateral surfaces of the parabasisphenoid. It extends along the entire anteroposterior length of the main body of the bone, starting at the anterior margin of the anterior tympanic recess and becoming confluent with the basisphenoid component of the basal tubera posteriorly.

The left and right basiptyergoid processes were recovered separated from the braincase, but the former was glued to the parabasisphenoid prior to scanning (Figs. 2, 3). Although the break is not clean, it was possible to determine the original position and orientation of the process. With the cultriform process horizontally aligned, the basiptyergoid process projects anteroventrally, and its anterior margin forms a 60° angle with the ventral surface of the cultriform process in lateral view. An anteroventrally oriented basiptyergoid process is also observed in

Lesothosaurus diagnosticus and *Efraasia minor*, whereas it is posteroventrally oriented in *Plateosaurus engelhardti*, and vertical in *Tawa hallae*. It is sometimes difficult to orient the whole braincase with precision, which can lead to imprecise morphological interpretations. Using the angle between the basiptyergoid and cultriform processes reduces this problem, improving our ability to recognize phylogenetically informative variation in the orientation of the basiptyergoid process (Bronzati and Rauhut, 2017).

The basiptyergoid process of MCP 3845-PV also has a lateral projection, forming an angle of 45° to the sagittal plane. Thus, left and right processes would form an angle of 90° to one another. The basiptyergoid process is 7.5 mm long and has a maximum width of 6 mm. It has a lanceolate shape in lateral view, being wider proximally and gradually narrowing distally. Its outer surface is irregular, with alternate concave and convex regions. Yet, it is generally slightly compressed mediolaterally and thicker at its posterior margin than anteriorly. This condition resembles that in *Lewisuchus admixtus*, which may be considered an intermediate state between the more laminar process of *Eodromaeus murphi*, *Tawa hallae*, and *Silesaurus opolensis* and the more rounded shape in sauropodomorphs such as *Plateosaurus engelhardti* and *Thecodontosaurus antiquus* (Benton et al., 2000).

The main body of the parabasisphenoid bears a large excavation on its lateral surface (Fig. 2), considered here to be the anterior tympanic recess (sensu Witmer, 1997). In dinosaurs, this recess usually extends from the anteroventral to the posterodorsal portion of the parabasisphenoid, invading the ventral margin of the lateral surface of the prootic (Rauhut, 2004; Sampson and Witmer, 2007; Bronzati and Rauhut, 2017). In MCP 3845-PV, the boundary between the parabasisphenoid and the prootic is not clear, but the dorsal edge of the recess is located directly ventral to the lateral opening for the facial nerve (but see below), indicating that the recess also invades the prootic. In contrast to *Thecodontosaurus antiquus* and *Efraasia minor*, in which the recess forms a single and continuous excavation, two distinct excavations are clearly visible in the anterior tympanic recess of *Saturnalia tupiniquim* (resembling the condition seen in *Lewisuchus admixtus*). The recess has a maximum length of 9 mm and a maximal width of 3 mm. Its anteroventral portion is elliptical and corresponds to approximately two-thirds its total length. It is bordered by the ventrolateral crest described above. The posterodorsal portion of the recess is shallower and has only half the size of the anteroventral portion. The cerebral branch of the internal carotid artery in dinosaurs typically enters the endocranial cavity through an aperture in the anteroventral portion of the anterior tympanic recess (Sampson and Witmer, 2007). Such a foramen is not visible in *Saturnalia tupiniquim*, but this may be an artifact (see below).

Posterior to the anterior tympanic recess, the posteroventral corner of the parabasisphenoid has a large depression on its lateral surface (Fig. 2) that we identify as the semilunar depression (see Discussion, below). The surface between the semilunar depression and the anterior tympanic recess is better preserved on the left side of the braincase. The ventral limit of the semilunar depression is clearly delineated by a 1-mm-thick, anteroposteriorly extending lamina, which also marks the lateral edge of the ventral surface of the parabasisphenoid. The recess is well defined posteriorly by a gently rounded ridge (2.5 mm thick) that also marks the transition between the lateral and posterior surfaces of the parabasisphenoid. The dorsal limit of the depression is located ventral to the fenestra, with the parabasisphenoid forming the ventral margin of this aperture. Anteriorly, there is no clearly marked limit, but the depression gets shallower until the level of the posterior margin of the anterior tympanic recess.

The pituitary fossa lies posterior to the cultriform process in the dorsal surface of the parabasisphenoid (Figs. 3, 4). The fossa has a

‘V’ shape in anterior view, with a rounded ventral margin. It is bordered posteriorly by a vertical, 1-mm-thick wall, the dorsum sellae. The medioventral portion of the fossa is usually perforated by the cerebral branches of the internal carotid arteries. As noted above, it is not possible to reconstruct the entire path of these canals in MCP 3845-PV. The CT data (Fig. 5) reveal two circular structures that we interpret as the internal carotid canals. Thus, we consider the absence of foramina in the pituitary fossa and in the anterior tympanic recess as most likely an artifact, caused by the preservation and/or the CT scan segmentation, rather than a condition deviating from that of all other dinosauriforms (e.g., Nesbitt, 2011; Bittencourt et al., 2014), with the exception of *Silesaurus opolensis* (Nesbitt, 2011; Piechowski et al., 2018).

Dorsal to the pituitary fossa (Fig. 4), a perforation corresponds to the passage of cranial nerve VI (= abducens nerve). Typically, the left and right nerves have independent apertures. Indeed, on the left side, it is possible to see that the dorsal part of the wall curves ventrally, almost reaching a dorsal projection from the ventral margin, which would have enclosed the nerve. An additional foramen between those for the abducens nerves is present in *Plateosaurus engelhardti* and has been associated with the basilar artery (Galton, 1985; but see Rauhut et al., 2010, for a discussion of the soft tissues associated with this foramen in dinosaurs). The presence/absence of this foramen cannot be determined in MCP 3845-PV due to the preservational quality of the specimen. An additional foramen is not present in the silesaurid *Silesaurus opolensis*.

Prootic—Left and right prootics of MCP 3845-PV are preserved in their entirety but largely covered with matrix (Figs. 2, 3). Only the posterolateral portion of the right prootic is exposed. Contacts with other bones include the parabasisphenoid ventrally, the otocipital posteriorly, the laterosphenoids anteriorly, and the

supraoccipital mediodorsally. The prootic forms or contributes to a series of structures in all dinosauriforms analyzed for this study, namely, the floccular fossae lobe (sensu Ferreira-Cardoso et al., 2017), preotic pendant, fenestra ovalis, dorsal tympanic recess, and foramina for trigeminal and facial nerves.

Immediately dorsal to the anterior tympanic recess (Fig. 2), the lateral surface of the braincase accepts the M. protractor pterygoideus (Holliday and Witmer, 2008). This attachment surface is typically formed by the prootic dorsally, with a contribution from the parabasisphenoid ventrally (Sampson and Witmer, 2007; Bronzati and Rauhut, 2017; Chapelle and Choiniere, 2018), but we could not positively identify this suture in MCP 3845-PV. The surface extends from the proximal part of the cultriform process (anteroventrally) to the ventral margin of the trigeminal notch (posterodorsally). It has a subrectangular shape, with a maximum length of 13 mm and maximum and minimum widths of 7 and 4 mm, respectively, at its dorsal-most and ventral-most portions. As observed in *Efraasia minor*, MCP 3845-PV does not have a well-developed preotic pendant. Accordingly, the ventral margin of the surface mainly follows the curvature of the dorsal portion of the anterior tympanic recess (Fig. 2). In some theropods, the preotic pendant forms a laminar structure covering part of the anterior tympanic recess in lateral view (Rauhut, 2004; Sampson and Witmer, 2007; Paulina-Carabajal and Currie, 2012). Additionally, in the sauropods *Diplodocus* and *Camarasaurus*, the anterior tympanic recess is completely obscured by the preotic pendant due to the relatively small size of the former (Paulina-Carabajal, 2015). Regarding early dinosauriforms, a relatively well-developed lamina covering part of the anterior tympanic recess in lateral view is also observed in *Eodromaeus murphi*. In *Tawa hallae*, the preotic pendant also forms a lamina, but one that projects less posteroventrally than in *E. murphi*. In contrast, the preotic pendant of *Silesaurus opolensis* is more robust and rounded, resembling the condition of sauropodomorphs such as *Plateosaurus engelhardti* and *Massospondylus carinatus* (Bronzati and Rauhut, 2017).

Dorsal to the region of the preotic pendant, a notch (Fig. 2) corresponds to the ventrolateral borders of the trigeminal foramen. The notch is elongated and ‘U’-shaped, with the anterior margin located slightly more medial than the posterior margin (Fig. 3). Its dorsal margin is 7.2 mm long and relatively straight for most of its length but curves slightly anteroventrally at its anterior third. The ventral margin of the notch is shorter (5.1 mm) and curves slightly dorsally at its anterior end. The notch has a width of 3.2 mm that is relatively constant along its length. The anteriorly placed laterosphenoid would have completed the notch as the trigeminal foramen (see below). Because the prootic-parabasisphenoid suture is unclear in this area, we presume that the ventral border of the foramen is formed by the prootic based on the observations of other dinosauriform taxa (*Tawa hallae*, *Panphagia protos*, *Massospondylus carinatus*, and *Pantydraco caducus*).

A previously discussed feature concerns the arrangement of the trigeminal nerve and middle cerebral vein as they exit the lateral braincase wall (e.g., Nesbitt, 2011; Bronzati and Rauhut, 2017). Three distinct morphologies are recognized. Separate foramina are found in some neotheropods (Rauhut, 2003), whereas a single foramen conveying both structures characterizes such forms as the sauropodomorph *Coloradisaurus brevis* (Apaldetti et al., 2014). The third condition is a partially divided notch in the prootic, with the vein occupying a more posteromedial position (Nesbitt, 2011; Bronzati and Rauhut, 2017), as observed in sauropodomorphs such as *Efraasia minor* and *Plateosaurus engelhardti*. Specimen MCP 3845-PV exhibits the first morphology with a single, elongate foramen that presumably conveyed the nerve and vein (Figs. 2, 3)—this is evident when the disarticulated left laterosphenoid is placed together with the rest of the braincase in a three-dimensional (3D) printed version of the specimen.

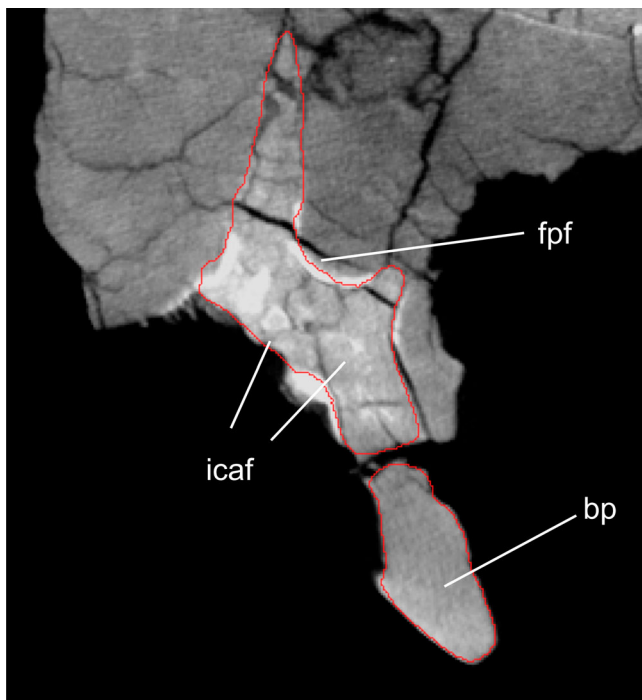


FIGURE 5. X-ray slice (coronal view) obtained from the CT scanning of the specimen MCP 3845-PV of *Saturnalia tupiniquim* showing the foramina associated with the internal carotid artery at the anteroposterior level of the pituitary fossa. **Abbreviations:** bp, basipterygoid process; fpf, floor of the pituitary fossa; icaf, foramina interpreted as the internal carotid artery.

Posteroventral to the trigeminal notch on both sides of the braincase, MCP 3845-PV bears a small circular foramen (Fig. 2), most likely formed by the facial nerve (CN VII). Its position relative to the anterior tympanic recess varies among dinosaurs. In *Panphagia protos* (Martínez et al., 2012b:fig. 8c) and *Tawa hallae* (M.B., pers. observ.), the facial foramen lies outside the anterior tympanic recess but near its dorsal margin. The foramen of *Lewisuchus admixtus*, in contrast, lacks clear separation from the recess, being either within or confluent with its dorsal limit (Bittencourt et al., 2014:fig. 4a). Specimen MCP 3845-PV exhibits bilateral asymmetry, with the left side having the condition of *P. protos* and *T. hallae* and the right side that of *L. admixtus*.

Below, we describe the different morphologies of the two sides, which could be the original condition of the braincase or the result of biases in preservation and/or segmentation of the CT data.

On the left side of the braincase, the foramen has a diameter of 0.8 mm and is separated from the anterior tympanic recess by a 1-mm surface that forms the dorsal roof of the recess (Fig. 2). A depression in the lateral surface of the prootic most likely corresponds to the path of the palatine ramus of CN VII, which turns anteroventrally after leaving the braincase (Galton, 1985; Sampson and Witmer, 2007). Likewise, a depressed surface between the two anterior rami of the otosphenoidal crest (sensu Sampson and Witmer, 2007) probably represents the path of the hyomandibular ramus of CN VII on the lateral surface of the prootic (Fig. 2); this surface turns posterolaterally after leaving the braincase (Galton, 1985; Sampson and Witmer, 2007). On the right side of the braincase, the surface between the trigeminal notch and the foramen is twice the length of that of the left side (2 mm), but the ventral margin of the foramen is confluent with the dorsal portion of the tympanic recess. Finally, regardless of the existence of these two alternative morphologies, neither side of the braincase of MCP 3845-PV bears a lamina partially covering the foramen in lateral view, as seen in *Lewisuchus admixtus* and *Panphagia protos* (Martínez et al., 2012b:fig. 8a, c). The lamina also appears absent in *Tawa hallae*.

We refer to the ridge on the dorsolateral surface of the braincase as the otosphenoidal crest (Sampson and Witmer, 2007) rather than crista prootica, because it can be formed by three different bones: the prootic, the otoccipital, and the parabasisphenoid. It is not possible to clearly establish the limits between the prootic and the otoccipital in MCP 3845-PV, but the otosphenoidal crest seems to have an otoccipital component that extends to the proximal portion of the paroccipital process (Fig. 2). Typically, the prootic overlaps the otoccipital at their contact, but this is not clear in MCP 3845-PV. The otosphenoidal crest is low and rounded (3 mm thick) in this region, extending anteriorly from its posterior tip for 8.5 mm before bifurcating at the level of the fenestra ovalis. The ventral branch forms the anterior margin of that fenestra and contacts the parabasisphenoid ventrally, thus marking the boundary between the fenestra ovalis and the anterior tympanic recess. The dorsal branch forms the dorsal margin of the facial foramen. It is important to stress that we treat both rami of the otosphenoidal crest as part of this structure because no discontinuity between them and the posterior-most portion of the crest is seen (Sobral et al., 2016; Bronzati and Rauhut, 2017).

Dorsal to the otosphenoidal crest, the prootic contacts the supraoccipital dorsally, the otoccipital posteriorly, and the laterosphenoid anteriorly (Figs. 2, 3). A large depression (topologically equivalent to the dorsal tympanic recess of Witmer, 1997) runs from the paroccipital process posteriorly to the trigeminal notch anteriorly, which represents ca. 60% of the lateral surface of the braincase. The ventral margin of the recess is rounded, giving a half-moon aspect to the whole structure in lateral view (Figs. 2–4). Its anterior limit is more sharply defined on the left side,

where a flat, triangular surface of bone separates the recess from the posterior margin of the trigeminal nerve notch. The anterior margin of the recess is vertical, extending from the otosphenoidal crest ventrally to the prootic margin, which would probably contact the parietal/laterosphenoid dorsally. On the right side, the recess is anteriorly shallow and not so sharply defined. It becomes even shallower dorsally, but it is not clear if it would also have excavated the parietal (Witmer, 1997). Finally, the recess is continuous on the left side of the braincase but bears two deeper regions separated by a low and thick swelling on the right. This crest extends from the dorsal margin of the stapedial groove to the portion of the prootic/otoccipital that contacts the anterodorsal surface of the supraoccipital.

The medial surface of the prootic housed the cerebral portion of the endocranial cavity (Bronzati et al., 2017) and is thus dorsoventrally concave (Fig. 4). A large and deep floccular recess (= auricular recess of some authors, e.g., Nesbitt, 2011) dominates the medial surface of the prootic (Fig. 4).

Otoccipital—Both otoccipitals are preserved with their lateral surfaces partially exposed. Both are missing the distal ends of their paroccipital processes (Figs. 2–4). The otoccipital-basioccipital contact is visible in the exposed occipital condyle, but otherwise its sutural contacts cannot be precisely identified. The dinosaur otoccipital usually contacts the supraoccipital dorsomedially, the parabasisphenoid anteroventrally, the basioccipital posteroventrally, and the prootic anterodorsally (Galton, 1984; Sampson and Witmer, 2007).

The otoccipital can be roughly divided into a dorsal portion that contacts the supraoccipital medially and the prootic anteriorly, and three projections that originate from this dorsal portion. One of these is the paroccipital process, which originates in the posterolateral corner of the bone. Ventromedial to the paroccipital process, a more robust projection forms the margins of the foramen magnum and occipital condyle, enclosing the foramina for the hypoglossal nerve. Anteroventrally, the crista interfenestralis forms the third projection, which separates the metotic foramen from the fenestra ovalis. The posterodorsal region of the braincase, formed by the otoccipital and supraoccipital, will be discussed separately, because the related bone limits are not at all clear (Figs. 2–4).

From the projection of the otoccipital that contributes to the foramen magnum described above, a smaller, additional posterior projection abuts the basioccipital portion of the condyle laterally. This projection is pyramidal and 5 mm long. Medially, it contributes to the floor of the endocranial cavity, forming its posterolateral edge. The ventral surface is flat at the contact with the basioccipital, whereas the dorsal surface is concave and antero-dorsally confluent with the portion of the otoccipital forming the lateral margins of the foramen magnum.

The total participation of the otoccipital in the borders of the foramen magnum cannot be precisely determined, because its suture to the supraoccipital is not discernible. However, in all the examined taxa where this contact is visible (e.g., *Lewisuchus admixtus*, *Plateosaurus engelhardti*), the otoccipital forms the lateral margin and at least part of the dorsal margin of the foramen. In MCP 3845-PV, the medial surface of the otoccipital that borders the foramen magnum extends ventromedially to dorsolaterally from the ventral limit of the foramen magnum, and dorsally it curves medially (Fig. 4). This change in orientation is especially marked, forming an angle of ca. 100° and resembling the morphology of *L. admixtus* and *Silesaurus opolensis* (see Bittencourt et al., 2014:fig. 3). The lateral margins of the foramen magnum of *Herrerasaurus ischigualastensis* and *P. engelhardti* are more gently rounded.

Anterior to the above pyramidal projection, the ventral portion of the otoccipital is pierced by two hypoglossal foramina (CN XII) recognizable only on the right side (Fig. 2). Both foramina are circular, the posterior being slightly larger than the anterior

(2 versus 1.5 mm diameter). The posterior foramen is also more dorsal, with its ventral margin on the same level as the dorsal margin of the anterior foramen. Dorsal to the hypoglossal foramina, an additional fossa lies posterior to the metotic foramen. However, the presence of an additional foramen in this area, which could indicate a division of the metotic foramen (Gower and Weber, 1998; Bronzati and Rauhut, 2017), remains uncertain.

Anterior to the foramina for the hypoglossal nerve, two larger apertures are seen in the lateral wall of the braincase (Fig. 2), the posterior of which is identified as the metotic foramen (Gower and Weber, 1998; Sobral et al., 2012; Bronzati and Rauhut, 2017), whereas the anterior corresponds to the fenestra ovalis (fenestra vestibuli). They are divided by a lateromedially expanded (3 mm) sheet of bone, the crista interfenestralis (Säve-Söderbergh, 1947; Sampson and Witmer, 2007). On the left side, where it is better preserved, the preserved dorsal portion of the crista is 5 mm high, but we estimate a total height of 7 mm. As in other dinosaurs, the crista interfenestralis has its dorsal tip at the ventral surface of the proximal portion of the paroccipital process, where both structures are confluent. From the paroccipital process, the crista extends anteroventrally. It is curved, with concave anterior and convex posterior margins.

The fenestra ovalis is of about the same size as the metotic foramen (Fig. 2), resembling the condition of *Plateosaurus engelhardti* and *Efraasia minor*. If the cultriform process is horizontally positioned, the fenestra ovalis is not strictly vertical but has its ventral margin located anterior to the dorsal margin. The anterior limit of the fenestra ovalis is defined by the anteroventral ramus of the otosphenoidal crest as described above. The dorsal margin of the fenestra has a depression that extends posteriorly until the

proximal portion of the paroccipital process, which is here identified as the stapedia groove (Fig. 2).

The paroccipital process projects posterolaterally from the dorsal margin of the otoccipital (Figs. 2–4). In taxa such as *Silesaurus opolensis*, *Tawa hallae*, and *Plateosaurus engelhardti*, the stapedia groove extends for only a short length of the paroccipital process. In MCP 3845-PV, the stapedia groove extends along the entire anteroventral margin of the paroccipital process as preserved. Yet, because only the proximal portion of this structure is present, it is not possible to estimate the total length of the groove.

Otoccipital and Supraoccipital: Posteromedial Region of the Dorsal Portion of Braincase—The dorsal margin of the foramen magnum of archosaurs is typically formed by the supraoccipital medially and the otoccipitals laterally (Nesbitt, 2011), but the contribution of each bone cannot be defined in MCP 3845-PV. The dorsal surface of the braincase anterior to the dorsal margin of the foramen magnum is transversely convex, mainly following the curvature of the foramen magnum and of the corresponding endocranial cavity (Fig. 4). Based on comparisons with *Silesaurus opolensis*, *Lewisuchus admixtus*, and *Plateosaurus engelhardti*, in which both bones are preserved in articulation, the region with a more marked dorsoventral inclination in MCP 3845-PV probably corresponds to the supraoccipital. With the cultriform process horizontally aligned, the dorsal margin of the supraoccipital forms an angle of ca. 70° in relation to the horizontal plane at its anterior portion (Fig. 2). A thick supraoccipital crest extends anteroposteriorly for half the length of the supraoccipital dorsal surface, starting at its anterior edge, along the midline of the bone. Lateral to this crest, the dorsal surface of the braincase is slightly concave transversely, as defined by its dorsally raised lateral margins (Fig. 4).

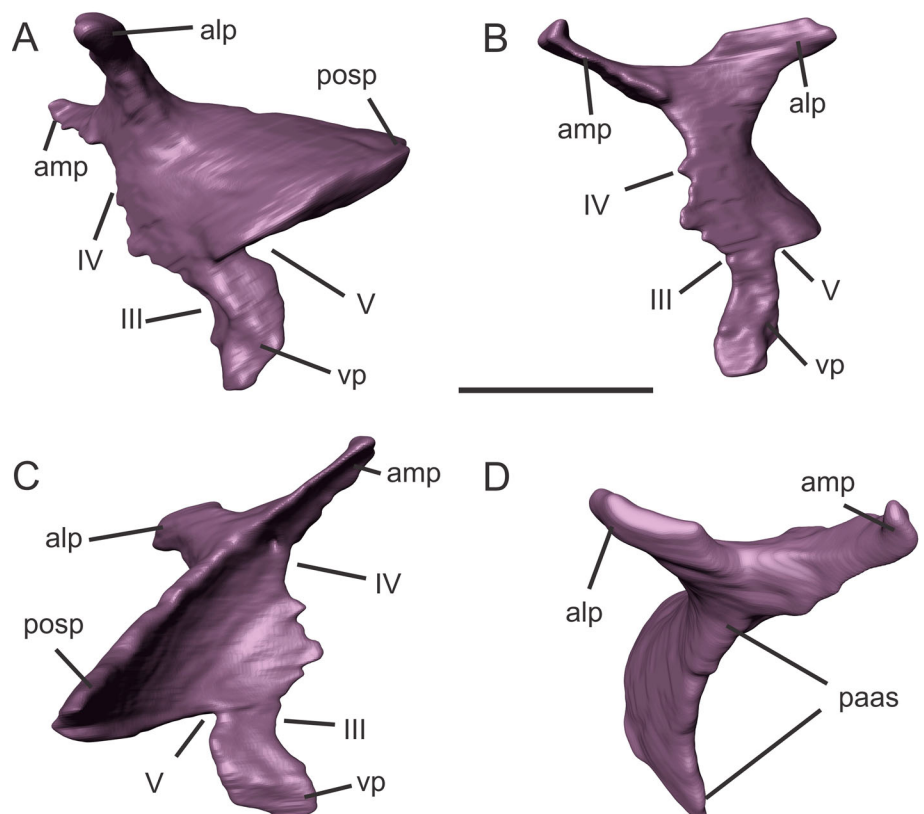


FIGURE 6. Three-dimensional reconstruction of the left laterosphenoid of the specimen MCP 3845-PV of *Saturnalia tupiniquim* in lateral (A), anterolateral (B), medial (C), and dorsal (D) views. **Abbreviations:** alp, anterolateral process; amp, anteromedial process; paas, articular surface with the parietal; posp, posterior process; vp, ventral process; III, path of the oculomotor nerve; IV, path of the trochlear nerve; V, path of the trigeminal nerve. Scale bar equals 1 cm.

Laterosphenoid—Both laterosphenoids are preserved isolated inside the block containing the other braincase bones. The right element lacks some of its processes, but the left is complete (Fig. 6). Because the preserved portions of both bones show no differences, this description is based solely on the left element. The laterosphenoid forms the anterodorsal portion of the braincase. It can be roughly divided into a central main body, which probably contacted the orbitosphenoid (if present) anteriorly, and four projections contacting other adjacent bones. The posterior process would have contacted the prootic, the anterolateral process the postorbital, the anteromedial process the frontal, and the ventral process the prootic or/and the parabasisphenoid.

The lateral surface of the main body of the laterosphenoid is dorsoventrally and anteroposteriorly concave, and its corresponding medial surface, which encloses the cerebral hemispheres as in other dinosaurs, is convex (Fig. 6). This is similar to the condition observed in other sauropodomorphs, such as *Plateosaurus engelhardti*, *Efraasia minor*, and *Massospondylus*, and in the saurischian *Tawa hallae*. The convex medial surface of the laterosphenoid of MCP 3845-PV forms the anterodorsal portion of the endocranial cavity and might have contacted the orbitosphenoid anteriorly, but this bone is not preserved or not ossified.

The ventral process represents slightly less than one-third the total height of the laterosphenoid (Fig. 6). Its posterior margin forms, together with the ventral margin of the posterior process of the bone, the dorsal margin of the trigeminal foramen (possibly conveying CN V and the lateral branch of the mid-cerebral vein; see above). The transition between these two processes forms a sharp angle.

The anterior margin of the ventral process is slightly convex. It merges with the main body of the bone dorsally, forming an indentation that corresponds to the passage of the oculomotor nerve (CN III). Dorsal to that, the anterior margin of the main laterosphenoid body is also concave, forming the posterior margin of the passage of the trochlear foramen for CN IV, below the anteromedial process. The anterior projection of the laterosphenoid margin, which separates the oculomotor and trochlear foramina, probably contacted the orbitosphenoid anteriorly (Chapelle and Choiniere, 2018).

Dorsal to the trochlear foramen, the anterior margin of the laterosphenoid gives rise to a lateromedially compressed process that projects dorsomedially and probably contacted the ventral surface of the frontal (Fig. 6). This process is as long as the ventral process described above. Other sauropodomorphs, such as *Plateosaurus engelhardti* (AMNH 6810) and *Massospondylus carinatus*, have a relatively shorter anteromedial process, less than half the length of the ventral process—although it may be incompletely preserved in the above-referred specimen of *P. engelhardti* (Prieto-Marquez and Norell, 2011). Given the length of those processes, it is possible that their tips contacted one another ventral to the frontal in MCP 3845-PV, similar to the condition observed in some theropods such as *Allosaurus* (O.W.M.R., pers. observ.).

The anteromedial and anterolateral laterosphenoid processes diverge at an angle of approximately 150° in dorsal view (Fig. 6). The anterolateral process, which contacted the postorbital, is rounded and slightly shorter than the anteromedial process. From the anterolateral process to the posterior process, the dorsal margin of the laterosphenoid would have contacted the anterior body of the parietal.

DISCUSSION

Here, we discuss braincase features relevant to the phylogeny of early dinosaurs and dinosauriforms (Nesbitt et al., 2009; Nesbitt, 2011; Bittencourt et al., 2014; Cabreira et al., 2016;

Baron et al., 2017; Bronzati and Rauhut, 2017). Because of the high level of disagreement among the recent phylogenetic hypotheses proposed (Langer, 2014; Baron et al., 2017; Langer et al., 2017), we chose to discuss dinosauriform braincase evolution by examining particular anatomical traits under distinct phylogenetic arrangements. Proposing a new phylogenetic hypothesis for dinosauriforms is beyond the scope of this work.

Recesses

We supplement the overview of Witmer (1997) on the pneumatic recesses of the dinosaur skull by focusing on early dinosaurs and non-dinosaurian dinosauriforms and discussing some nomenclatural issues.

Subsellar Recess—The sellar recess is located on the ventral surface of the proximal portion of the cultriform process of the parabasisphenoid (Witmer, 1997). It is present in all examined dinosauriforms in which that area is preserved and visible (Fig. 7) and thus likely plesiomorphic for dinosaurs. Regarding the ancestral condition for dinosauriforms, a depression is observed in the non-archosaurian archosauriform *Prolacerta broomi* and in the non-saurian diapsid *Youngina capensis* (Gardner et al., 2010:fig. 5). In both taxa, the recess is divided by a median ridge as in *Silesaurus opolensis* (see below).

Regarding the three main dinosaur lineages, a sellar recess is widespread among theropods (Rauhut, 2004; Witmer and Ridgely, 2009; Bever et al., 2013). Recently, Bronzati and Rauhut (2017) mentioned that the term had not been used in the sauropodomorph literature, but that the structure is common to all sauropodomorphs. In Ornithischia, a recess at the ventral base of the cultriform process is present in *Hypsilophodon foxi* and *Dysalotosaurus lettowvorbecki* (Sobral et al., 2012:fig. 1b). A sellar recess seems to be absent in one specimen of *Lesothosaurus diagnosticus* (NHMUK PV RU B17) but is clearly present in another (NHMUK PV R8501). The absence of a sellar recess was reported for ankylosaurid ornithischians (Paulina-Carabajal et al., 2018) and for the megaraptoran theropod *Murusraptor barrosaensis* (Paulina-Carabajal and Currie, 2017). Nevertheless, the presence or absence of the sellar recess does not inform the relationships of early dinosauriforms.

Two characters related to the sellar recess were proposed by Bronzati and Rauhut (2017) in the context of sauropodomorph evolution. One of these is related to the ridges that extend on the ventral surface of the cultriform process. In *Saturnalia tupiniquim*, these ridges originate from the lamina connecting the cultriform and basiptyergoid processes and extend parallel to one another until they fade away anteriorly. Thus, the sellar recess is not as clearly defined anteriorly, similar to the condition observed in *Massospondylus carinatus*. In *Plateosaurus engelhardti* and *Lewisuchus admixtus*, the ridges converge anteriorly on the ventral surface of the parabasisphenoid, giving a triangular aspect to the anterior margin of the recess. On the other hand, the ridges of *Silesaurus opolensis* extend parallel to one another, as in *S. tupiniquim*, but instead of merging with the ventral surface of the cultriform process, they extend along the dorsal portion of the lateral surface of the cultriform process. Unfortunately, the proximal portion of the cultriform process is not visible or preserved in many of the examined specimens (*Herrerasaurus ischigualastensis*, *Eoraptor lunensis*). A second character discussed by Bronzati and Rauhut (2017) deals with the depth/width ratio of the sellar recess. For instance, taxa such as *Eocursor parvus* and *Lesothosaurus diagnosticus* exhibit a ‘shallow’ recess, with the total width greater than the dorsoventral depth. On the other hand, *Efraasia minor* and *Tawa hallae* have a ‘deep’ recess, which is at least as deep as wide (Fig. 7).

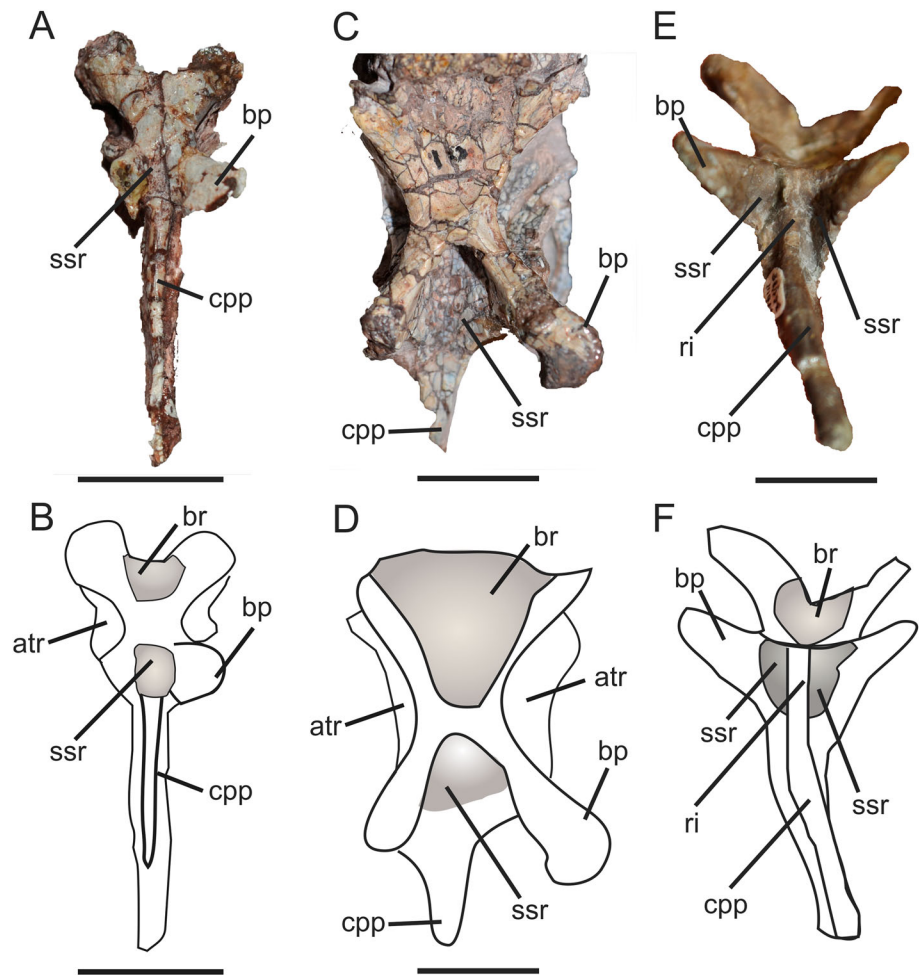


FIGURE 7. Parabasisphenoid of the specimens SAM-PK-K8025 of *Eocursor parvus* (A, B), SMNS 12667 of *Efraasia minor* (C, D), and ZPAL Ab III/361 of *Silesaurus opolensis* (E, F), in anteroventral views. **Abbreviations:** atr, anterior tympanic recess; bp, basipterygoid process; br, basisphenoid recess; cpp, cultriform process of the parabasisphenoid; ri, ridge; ssr, subsellar recess. Scale bars equal 1 cm.

Another trait with possible phylogenetic implications is the presence/absence of a ridge medially dividing the subsellar recess (Fig. 7). This ridge on the ventral surface of the parabasisphenoid corresponds to the ventral expression of the groove for the cartilaginous interorbital septum, which is located on the dorsal (internal) surface of the cultriform process of the parabasisphenoid (Gardner et al., 2010:fig.3). This ridge is present in the non-dinosauriforms *Silesaurus opolensis* and *Lewisuchus admixtus*, and also in other non-archosaurian diapsids such as *Prolacerta broomi* and *Youngina capensis*. In contrast, the ridge is not present in *E. minor* (Fig. 7) or other examined dinosaurs where this region is visible (*Tawa hallae*, *Massospondylus carinatus*, *PlatEOSaurus engelhardti*). In this case, if silesaurids do not belong to Ornithischia (Cabreira et al., 2016) and the presence of the ridge is plesiomorphic for Dinosauromorpha, the absence of such a ridge could be synapomorphic for Dinosauria. However, our small sampling of non-dinosaurian taxa hampers drawing more affirmative conclusions.

Basisphenoid Recess and ‘Median Pharyngeal Recess’—Posterior to the subsellar recess, another depression in the ventral surface of the parabasisphenoid corresponds to the basisphenoid recess of Witmer (1997). A series of subsequent studies (Gower, 2002; Martz and Small, 2006; Sobral et al., 2016) used the term ‘median pharyngeal recess’ to refer to a similarly positioned depression. Those authors often quote Witmer

(1997) as a reference, but the term ‘median pharyngeal recess’ does not appear in his work. Instead, Witmer (1997) mentions that the basisphenoid recess probably originates from a median pharyngeal system (also Witmer and Ridgely, 2009; Dufeau and Witmer, 2015), and a literature survey did not find any work referring to a ‘median pharyngeal recess’ before Witmer (1997). In this context, the use of the term ‘median pharyngeal recess’ might correspond to an equivocal interpretation of Witmer (1997), or to other interpretations of the authors not further clarified in their works. Other works have commented on the equivalence of the terms ‘basisphenoid recess’ and ‘median pharyngeal recess’ (Nesbitt, 2011; Ezcurra, 2016; Sobral et al., 2016). Here, we adopt the term ‘basisphenoid recess’ following the original formulation of Witmer (1997).

A basisphenoid recess is extensively reported for theropods (Bakker et al., 1988; Rauhut, 2003, 2004; Sampson and Witmer, 2007) and recently demonstrated as present in sauropodomorph dinosaurs (Bronzati and Rauhut, 2017) and at least some non-archosaurian archosauriforms (Sobral et al., 2016). Such a widespread distribution was already mentioned by Witmer (1997) and more recently by Dufeau (2011). In fact, a depression in the ventral surface of the basisphenoid, even if very subtle (*Lesothosaurus diagnosticus*, *Eocursor parvus*), was identified for all taxa analyzed for this study (Fig. 7). In contrast, Nesbitt (2011) stated that the recess is absent in the archosauriforms

Prolacerta broomi and *Euparkeria capensis* and in the dinosaurs *L. diagnosticus*, *Plateosaurus engelhardti*, and *Herrerasaurus ischigualastensis*. However, this difference between the interpretations is most likely the result of variation in the development of the recess in different taxa. For instance, the recess in non-archosaurian archosauriforms, such as *P. broomi* and *E. capensis* (Sobral et al., 2016), and some sauropodomorphs, such as *Efraasia minor* (Bronzati and Rauhut, 2017), is clearly not as well developed as that of some theropods such as *Megapnosaurus rhodesiensis* (Raath, 1985) and *Piatnitzkysaurus floresi* (Rauhut, 2004:fig. 7). In this context, a ‘less-developed’ recess might be coded as absent for some taxa, according to the interpretation of other authors (Nesbitt, 2011; Cabreira et al., 2016; Baron et al., 2017). Thus, the size/depth of the basisphenoid recess may be a better way to express such variation in a phylogenetic context. In this sense, the presence of a basisphenoid recess as synapomorphic for Ornithoscelida as proposed in Baron et al. (2017) is problematic for the above reasons.

Finally, Sobral et al. (2016) argued that Nesbitt (2011) scored the ‘median pharyngeal recess’ as absent in *Euparkeria capensis* due to different interpretations on what consists in the basisphenoid recess. According to these authors (Sobral et al., 2016:29), Nesbitt (2011) understood the recess as a “pronounced depression at the anterior extreme of the ventral fossa at the midline,” differing from the most widely used definition of the term. However, the pronounced depression mentioned by Sobral et al. (2016), i.e., that of character 107 in Nesbitt (2011), is not the basisphenoid recess (‘median pharyngeal recess’), but another depression in the basioccipital. Nesbitt (2011) deals with the basisphenoid recess (or ‘median pharyngeal recess’) in his character 100, which is clearly in accordance with the most used definition of the term (Witmer, 1997).

Recess in the Basioccipital—In his character 107, Nesbitt (2011) discusses the presence of a recess on the ventral surface of the basioccipital, which is illustrated by a foramen present in *Protosuchus richardsoni* and a deeper and wider recess of *Sphenosuchus acutus* (see Nesbitt, 2011:fig. 24a, e). It is important to mention that the phylogenetic character of Nesbitt (2011) set the recess at the basioccipital apart from the basisphenoid recess, because the latter is considered as exclusive to the basisphenoid.

One problematic aspect is setting apart the recess in the basioccipital from the one in the basisphenoid because the basisphenoid recess (sensu Witmer, 1997) fades away toward the anterior surface of the basioccipital (Fig. 8). Indeed, this morphology was observed in all taxa for which the basisphenoid recess is preserved and visible, such as the crocodylomorph *Sphenosuchus acutus*, the dinosauriform *Marasuchus lilloensis*, the silesaurid *Lewisuchus admixtus*, the sauropodomorphs *Buriolestes schultzi* (Fig. 8), *Efraasia minor*, *Plateosaurus*, *Massospondylus carinatus*, *Coloradisaurus brevis*, and theropods such as *Megapnosaurus rhodesiensis* (Fig. 8), *Fukuivenator paradoxus* (Azuma et al., 2016:fig. 4), and *Piatnitzkysaurus floresi* (Rauhut, 2004:fig. 3c). Additionally, in the theropods mentioned above and in *S. acutus*, the recess is well defined posteriorly at the level of the basioccipital and is divided by a ridge on the midline. This is congruent with the division of the posterior region of the cavity associated with the sinus as reported for neotheropods (Witmer and Ridgely, 2009). In this scenario, characters 100 (basisphenoid recess) and 107 (blind pit in the basioccipital) of Nesbitt (2011) might be non-independent in the context of early dinosauriforms, because the basisphenoid recess extends on the ventral surface of both basioccipital and parabasisphenoid. Nevertheless, a median ridge dividing the posterior portion of the basisphenoid recess is phylogenetically informative. For instance, taxa such as *Buriolestes schultzi* and *Lewisuchus admixtus* lack the ridge, whereas taxa such as *Megapnosaurus rhodesiensis* and *Sphenosuchus acutus* possess it.

Within the portion of the basisphenoid recess on the basioccipital, an additional blind pit is observed in taxa such as the saurischians *Buriolestes schultzi* (Fig. 8; rounded pit), *Massospondylus carinatus* (Fig. 8; SAM-PK-K1314; anteroposteriorly elongated pit), *Plateosaurus engelhardti* (AMNH 6810; anteroposteriorly elongated pit), *Plateosaurus* spp. (MB.R.5586.1; rounded pit), and *Eoraptor lunensis* (rounded pit) and the ornithischian *Hypsilophodon foxi* (Sobral et al., 2012). A blind pit seems to be present also in *Lewisuchus admixtus* and in one specimen of *Silesaurus opolensis* (ZPAL Ab III/361) but absent in another specimen of the latter (ZPAL Ab III/364). The situation is unclear in *Herrerasaurus ischigualastensis* because the contact between the basioccipital and the parabasisphenoid cannot be traced, but a single pit is observed anterior to the basal tubera in this taxon. A blind pit in the basioccipital is likely absent in *Efraasia minor* (but the anterior projection of the basioccipital is partially damaged) and in *Marasuchus lilloensis*.

One possibility is that this blind pit corresponds to further pneumatic expansions of basisphenoid diverticula of the median pharyngeal system (Dufeau and Witmer, 2015). If our interpretation is correct, even in the presence of further expansion, there is no connection between the median pharyngeal system and the pharyngotympanic sinus system in dinosauriforms. In contrast, crocodyliforms exhibit a connection between the two systems via the median pharyngeal tube (Dufeau and Witmer, 2015); this structure is present in *Protosuchus richardsoni*, which was interpreted by Nesbitt (2011) as possessing the basioccipital recess (character 107 of that study). However, the median pharyngeal tube (which connects the two systems) of crocodyliforms is here interpreted as nonhomologous to the portion of the basisphenoid recess located on the basioccipital, or to the blind pit on the basioccipital.

Anterior Tympanic Recess—The anterior tympanic recess (Figs. 2, 9) originates from diverticula of the middle ear sac and is located on the lateral surface of the parabasisphenoid, often extending onto the prootic, ventral to the facial foramen and otosphenoidal crest (Witmer, 1997). Its presence was recognized in all other dinosauriforms (Nesbitt, 2011) and recently was also identified in the lagerpetid *Ixalerpeton polesinensis* (Cabreira et al., 2016). Furthermore, Sobral et al. (2016) stated that the depression on the lateral surface of the parabasisphenoid of the non-archosaurian archosauriform *Euparkeria capensis* is topologically equivalent, hence homologous, to the anterior tympanic recess of dinosaurs (but see Gower and Weber, 1998). Thus, the presence/absence of an anterior tympanic recess (in the general sense discussed above) is noninformative for dinosauriforms because the structure is present in all taxa, as already indicated in Nesbitt (2011). As also pointed out by Nesbitt et al. (2011), the cerebral branches of the internal carotid artery can enter the braincase through the anterior tympanic recess, on the lateral side of the braincase as in dinosaurs, or ventrally, through the ventral surface of the parabasisphenoid as in *Silesaurus opolensis*. The condition observed in this taxon is similar to the one observed in non-archosaurian archosauriforms such as *Prolacerta broomi* and *Euparkeria capensis*. Nevertheless, given the lack of information for non-dinosaurian dinosauriforms, it is still not possible to state whether the condition of *S. opolensis* is ancestral for Dinosauria or it is a unique condition of *S. opolensis* among early dinosauriforms. Regarding later representatives of Dinosauria, a condition similar to the one of *S. opolensis* is observed among titanosaurs (Paulina-Carabajal, 2012, 2015).

Semilunar Depression

A detailed discussion on the non-archosaurian archosauriform semilunar depression is given by Gower and Weber

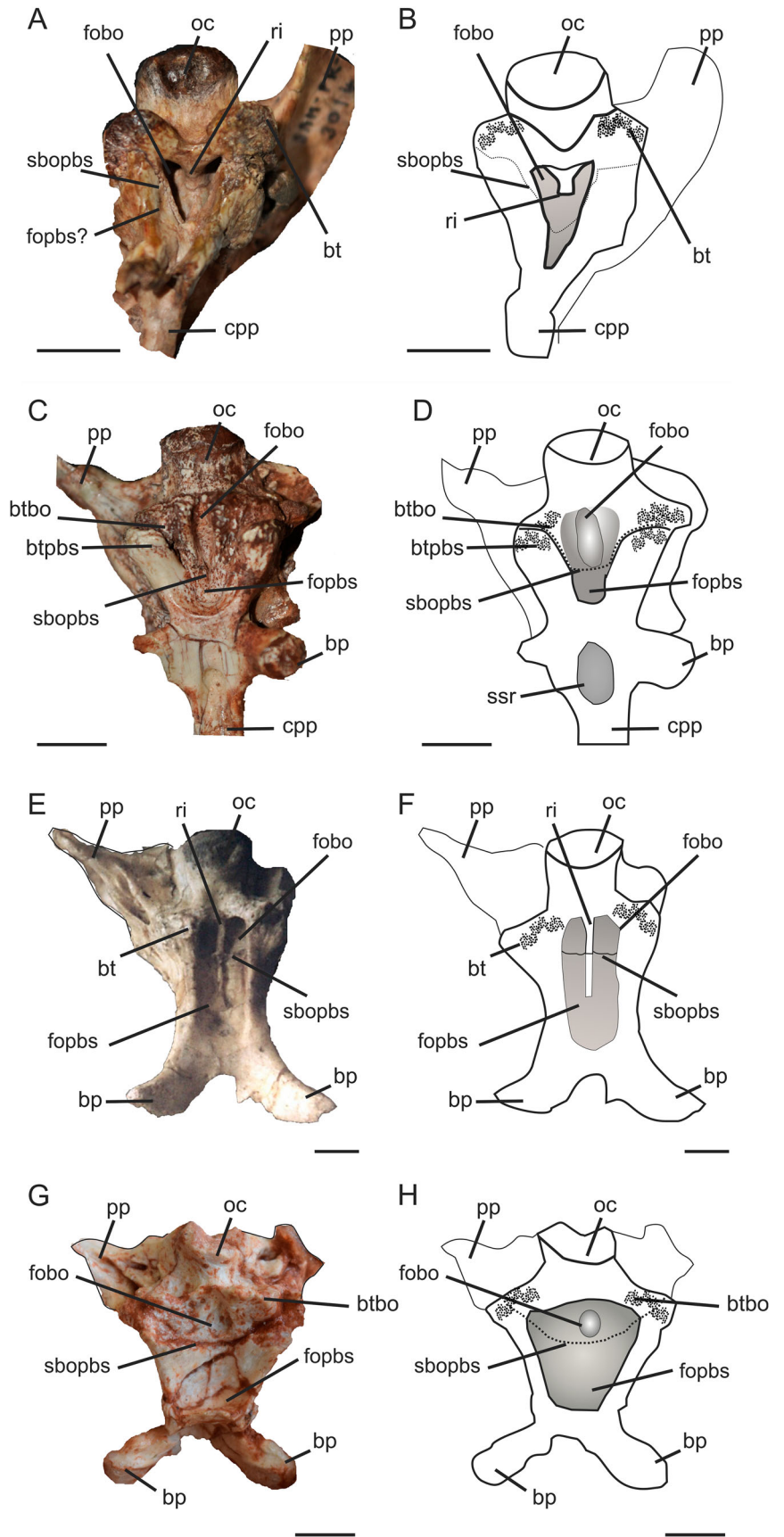


FIGURE 8. Parabasisphenoid and basioccipital of the specimens SAM 3014 of *Sphenosuchus acutus* (A, B), SAM-PK-K1314 of *Massospondylus carinatus* (C, D), QG 195 of *Megapnosaurus rhodesiensis* (E, F), and CAPPA/UFSM 0035 of *Buriolestes schultzi* (G, H) in ventral view. **Abbreviations:** bp, basipterygoid process; bt, basal tuber; btbo, basioccipital component of the basal tubera; btpbs, basisphenoid component of the basal tubera; cpp, cultriform process of the parabasisphenoid; fobo, fossa in the basioccipital; fopbs, fossa in the parabasisphenoid; oc, occipital condyle; pp, paroccipital process; ri, ridge; sbopbs, basioccipital-parabasisphenoid suture; ssr, subsellar recess. Scale bars equal 1 cm.

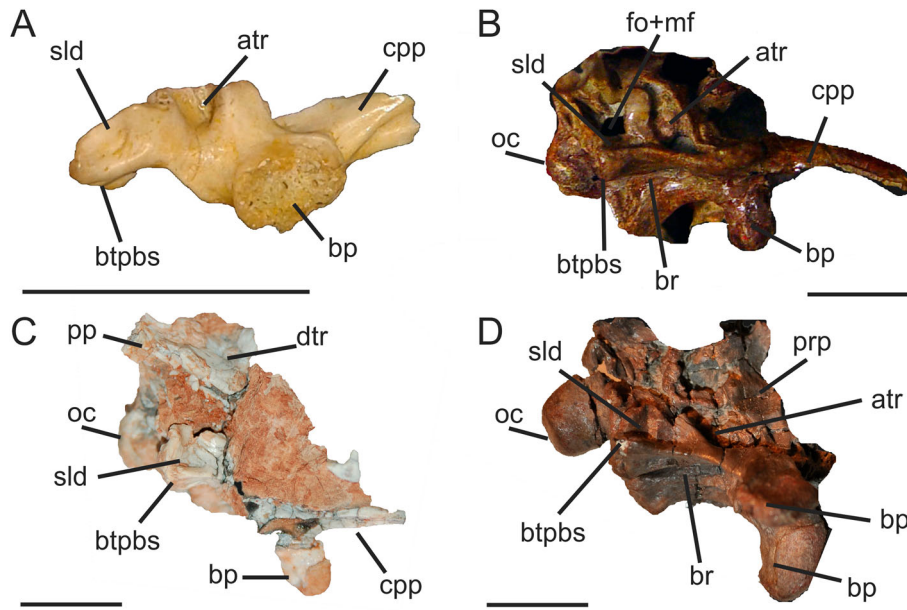


FIGURE 9. Parabisphenoid of the specimens ZPAL RV/413 of *Osmolskina czatkowiczensis* (A), PULR 01 of *Lewisuchus admixtus* (B), MCP 3845-PV of *Saturnalia tupiniquim* (C), and PVSJ 562 of *Eodromaeus murphi* (D) in lateral view. **Abbreviations:** atr, anterior tympanic recess; bp, basiptyergoid process; br, basi-sphenoid recess; btpbs, basisphenoid component of the basal tubera; cpp, cultriform process of the parabisphenoid; dtr, dorsal tympanic recess; fo + mf, fenestra ovalis and metotic foramen; oc, occipital condyle; pp, par-occipital process; prp, preotic pendant; sld, semilunar depression. Scale bars equal 1 cm.

(1998), where the authors homologized a depression on the lateral surface of the parabisphenoid of *Euparkeria capensis* with a similar structure previously identified by Evans (1998: figs. 1, 4) for the non-archosauriform archosauromorph *Prolacerta broomi*. According to Gower and Weber (1998), among non-archosaurian archosauriforms, this depression is consistently present on the posteroventral corner of the parabisphenoid, anterior (and/or dorsal; M.B., pers. observ.) to the basisphenoidal component of the basal tubera.

The presence/absence of a semilunar depression (Nesbitt et al., 2009; Nesbitt, 2011; Cabreira et al., 2016) was used in previous phylogenetic studies of early dinosaurs. However, it was scored as present in *Megapnosaurus kayentakatae* in Nesbitt et al. (2009), but later Nesbitt (2011) mentioned that this structure was absent in crown-group archosaurs. We did not analyze the braincase of *M. kayentakatae*, but a depression in the posteroventral corner of the lateral surface of the basisphenoid is present in *Megapnosaurus rhodesiensis*. Recently, a similar depression was reported for the lagerpetid *Ixalerpeton polesinensis* (Cabreira et al., 2016), and our observations indicate that such a depression is also present in non-dinosaurian dinosauriforms, such as *Marasuchus lilloensis* and *Lewisuchus admixtus*, as well as in the saurischians *Eodromaeus murphi* and *Saturnalia tupiniquim* (Figs. 2, 9). It is, however, absent in *Silesaurus opolensis*, *Herrerasaurus ischigualastensis*, *Tawa hallae*, *Efraasia minor*, *Plateosaurus engelhardti*, *Eocursor parvus*, and *Lesothosaurus diagnosticus*.

We remain largely ignorant regarding the presence of semilunar depressions in non-archosaurian archosauriforms, but the presence of this structure in *Euparkeria* and in the non-dinosaurian dinosauriforms *Ixalerpeton polesinensis* and *Marasuchus lilloensis* might indicate that it is the ancestral condition of Dinosauriformia. For Dinosauria, the presence of a semilunar depression in *Saturnalia tupiniquim* and *Eodromaeus murphi*, and its absence in taxa such as *Herrerasaurus ischigualastensis*, *Tawa hallae*, and *Buriolestes schultzi*, indicates a scenario of multiple acquisitions and/or losses of this structure, which is characteristic of pneumatic systems (Witmer, 1997). However, no correlation of this structure with a particular pneumatic system or with any other function

or soft tissue has been established so far (Gower, 1997). Finally, in contrast to the basisphenoid recess, we could not identify a shallow version of the semilunar depression in taxa purported to lack this feature.

Relative Position of the Ventral Braincase Elements

The relative position of some structures at the ventral margin of the braincase (i.e., the cultriform process of the parabisphenoid, basal tubera, and ventral limit of the occipital condyle) has been analyzed in the context of sauropodomorph (Yates, 2007; Chappelle and Choiniere, 2018) and early dinosauriform (Bittencourt et al., 2014) evolution. Regarding Sauropodomorpha, previous studies (Yates, 2007) have found that the plesiomorphic condition is the alignment of all these elements in nearly the same dorsoventral plane. Indeed, this is the condition assumed for taxa such as *Thecodontosaurus antiquus* (Benton et al., 2000) and *Pantyraco caducus*.

A problematic aspect of this character is that the sauropodomorph basal tubera are not a single and/or continuous structure, but a set of knobs and protuberances spanning the basioccipital and the parabisphenoid that have different positions in the dorsoventral axis (Bronzati and Rauhut, 2017). In *Thecodontosaurus antiquus*, for example, the basisphenoidal component of the basal tubera is at the same dorsoventral level of the ventral surface of the parasphenoid rostrum and the ventral limit of the occipital condyle, but part of its basioccipital component is dorsal to these elements. Thus, the ‘basal tubera complex’ as a whole does not represent a good landmark for analyzing variation in the alignment of those elements. Nevertheless, comparisons between the ventral surfaces of the occipital condyle and cultriform process are feasible. In this sense, *Saturnalia tupiniquim* has a stepped braincase, with the ventral surface of the cultriform process ventrally located in relation to the ventral limit of the occipital condyle (Fig. 2). This is the same morphology observed in other sauropodomorphs, such as *Plateosaurus engelhardti* and *Massospondylus carinatus*. On the other hand, *T. antiquus* has a braincase with the ventral limit of the occipital condyle at the same level as the ventral margin of the cultriform process,

which is the condition observed in *Lewisuchus admixtus* and *Lesothosaurus diagnosticus* (Porro et al., 2015).

Unfortunately, the relative position of these elements in other taxa is difficult to establish, because they are either hidden by other bones or not preserved in articulation. This hampers the elaboration of a more detailed scenario of morphological variation, but we believe that solely using the relative position of the cultriform process of the parabasisphenoid and the occipital condyle is a better approach than adding information on the basal tubera complex.

CONCLUSION

Computed tomography allowed a detailed investigation of the braincase anatomy of the Late Triassic sauropodomorph *Saturnalia tupiniquim*. The description provided here adds to previous publications focusing on the braincase anatomy of Late Triassic sauropodomorphs and enhances our understanding of this structure in early dinosaurs and their closest dinosauriform relatives. Regarding the recesses of the braincase, as mentioned by Witmer (1997), birds are the maximal exponents of skull pneumatization in archosaurs, but nonavian theropods also exhibit a well-developed pneumatic cranial system. Indeed, in comparison with other dinosaurs, the braincase recesses of theropods are more easily recognized, but various of these recesses, even if ‘less-developed,’ are also widespread among other dinosaurs and non-dinosaurian dinosauriforms. For instance, the basisphenoid and subsellar recess were also observed in all taxa analyzed for this study. Hence, the presence/absence of these structures is not phylogenetically informative at this taxonomic level, and the relative level of development should be used in the construction of phylogenetic characters. Our investigation also indicates that the semilunar depression of non-archosaurian archosauriforms is also present in some dinosaurs and non-dinosaurian dinosauriforms.

Finally, the phylogeny of early dinosauriforms is still in a state of flux (Ezcurra, 2010; Langer et al., 2010, 2017; Nesbitt et al., 2010; Martínez et al., 2011, 2012a; Langer and Ferigolo, 2013; Bittencourt et al., 2014; Cabreira et al., 2016; Baron et al., 2017). In this context, future studies might incorporate the information discussed here in the form of phylogenetic characters, which may help stabilize tree topologies and reveal a clearer pattern of dinosauriform braincase evolution.

ACKNOWLEDGMENTS

We are thankful to G. Rößner, B. Ruthensteiner, S. Lautenschlager, and D. Dufeu for assistance with CT imaging and scientific content. A. A. S. da Rosa, D. Schwarz, D. Abelin, G. Cisterna, H. Ketchum, J. Powell, J. Choniere, P. Barrett, R. Schoch, R. Martinez, S. Chapman, and Z. Erasmus helped and/or provided access to materials in collections, which we are thankful for. We are especially thankful to the reviewers A. Paulina-Carabajal and L. Witmer for their insightful comments. This work was supported by the Conselho Nacional de Desenvolvimento Científico e Tecnológico (CNPq) Science without Borders grant 246610/2012-3 to M.B. and grant 170867/2017-0 to M.B. and M.C.L., by the Fundação de Amparo à Pesquisa do Estado de São Paulo (FAPESP) grant 2014/03825-3 to M.C.L., and by the Deutsche Forschungsgemeinschaft (DFG) grant RA 1012/12-1 to O.W.M.R.

ORCID

Mario Bronzati  <http://orcid.org/0000-0003-1542-3199>

Max C. Langer  <http://orcid.org/0000-0003-1009-4605>

Oliver W. M. Rauhut  <http://orcid.org/0000-0003-3958-603X>

LITERATURE CITED

- Apaldetti, C., R. N. Martínez, D. Pol, and T. Souter. 2014. Redescription of the skull of *Coloradisaurus brevis* (Dinosauria, Sauropodomorpha) from the Late Triassic Los Colorados Formation of the Ischigualasto-Villa Union Basin, northwestern Argentina. *Journal of Vertebrate Paleontology* 34:1113–1132.
- Azuma, Y., X. Xu, M. Shibata, S. Kawabe, K. Miyata, and T. Imai. 2016. A bizarre theropod from the Early Cretaceous of Japan highlights mosaic evolution among coelurosaurians. *Scientific Reports* 6:20478.
- Bailleul, A. M., J. B. Scannella, J. R. Horner, and D. C. Evans. 2016. Fusion patterns in the skulls of modern archosaurs reveal that sutures are ambiguous maturity indicators for the Dinosauria. *PLoS ONE* 11: e0147687.
- Bakker, R. T., M. Williams, and P. Currie. 1988. *Nanotyrannus*, a new genus of pygmy tyrannosaur, from the latest Cretaceous of Montana. *Hunteria* 1:1–30.
- Baron, M. G., D. B. Norman, and P. M. Barrett. 2017. A new hypothesis of dinosaur relationships and early dinosaur evolution. *Nature* 543:501–506.
- Benton, M. J., L. Juul, G. W. Storrs, and P. M. Galton. 2000. Anatomy and systematics of the prosauropod dinosaur *Thecodontosaurus antiquus* from the Late Triassic of Southwest England. *Journal of Vertebrate Paleontology* 20:77–108.
- Bever, G. S., S. L. Brusatte, T. D. Carr, X. Xu, A. M. Balanoff, and M. A. Norell. 2013. The braincase anatomy of the Late Cretaceous dinosaur *Alioramus* (Theropoda: Tyrannosauroidae). *Bulletin of the American Museum of Natural History* 376:1–72.
- Bittencourt, J. S., A. B. Arcucci, C. A. Marsicano, and M. C. Langer. 2014. Osteology of the Middle Triassic archosaur *Lewisuchus admixtus* Romer (Chañares Formation, Argentina), its inclusivity, and relationships amongst early dinosauriforms. *Journal of Systematic Palaeontology* 13:189–219.
- Bronzati, M., and O. W. M. Rauhut. 2017. Braincase redescription of *Efraasia minor* Huene, 1908 (Dinosauria: Sauropodomorpha) from the Late Triassic of Germany, with comments on the evolution of the sauropodomorph braincase. *Zoological Journal of the Linnean Society* 182:173–224.
- Bronzati, M., O. W. M. Rauhut, J. S. Bittencourt, and M. C. Langer. 2017. Endocast of the Late Triassic (Carnian) dinosaur *Saturnalia tupiniquim*: implications for the evolution of brain tissue in Sauropodomorpha. *Scientific Reports* 7:11931.
- Bronzati, M., R. B. J. Benson, and O. W. M. Rauhut. 2018. Rapid transformation in the braincase of sauropod dinosaurs: integrated evolution of the braincase and neck in early sauropods? *Palaeontology* 61(2):289–302.
- Butler, R. J. 2010. The anatomy of the basal ornithischian dinosaur *Eocursor parvus* from the Lower Elliot Formation (Late Triassic) of South Africa. *Zoological Journal of the Linnean Society* 160:648–684.
- Cabreira, S. F., A. W. A. Kellner, S. Dias-da-Silva, L. R. Silva, M. Bronzati, J. C. A. Marsola, R. T. Müller, J. S. Bittencourt, B. J. Batista, T. Raugust, R. Carrilho, A. Brodt, and M. C. Langer. 2016. A unique Late Triassic dinosauriform assemblage reveals dinosaur ancestral anatomy and diet. *Current Biology* 26:3090–3095.
- Chapelle, K. E. J., and J. N. Choiniere. 2018. A revised cranial description of *Massospondylus carinatus* Owen (Dinosauria: Sauropodomorpha) based on computed tomographic scans and a review of cranial characters for basal Sauropodomorpha. *PeerJ* 6:e4224.
- Currie, P. J. 1997. Braincase anatomy; pp. 81–85 in P. J. Currie and K. Padian (eds.), *Encyclopedia of Dinosaurs*. Academic Press, San Diego, California.
- Currie, P. J., and X.-J. Zhao. 1994. A new troodontid (Dinosauria, Theropoda) braincase from the Dinosaur Park Formation (Campanian) of Alberta. *Canadian Journal of Earth Sciences* 30:2231–2247.
- Dufeu, D. L. 2011. The evolution of the cranial pneumaticity in Archosauria: patterns of paratympanic sinus development. Ph.D. dissertation. College of Arts and Sciences, Ohio University, Athens, Ohio, 174 pp.
- Dufeu, D. L., and L. M. Witmer. 2015. Ontogeny of the middle-ear air-sinus system in *Alligator mississippiensis* (Archosauria: Crocodylia). *PLoS ONE* 10:e0137060.

- Evans, S. E. 1986. The braincase of *Prolacerta broomi* (Reptilia, Triassic). Neues Jahrbuch für Geologie und Paläontologie, Abhandlungen 173:181–200.
- Ezcurra, M. D. 2010. A new early dinosaur (Saurischia: Sauropodomorpha) from the Late Triassic of Argentina: a reassessment of dinosaur origin and phylogeny. Journal of Systematic Palaeontology 8:371–425.
- Ezcurra, M. D. 2016. The phylogenetic relationships of basal archosauromorphs, with an emphasis on the systematics of proterosuchian archosauroid forms. PeerJ 4:e1778.
- Fedak, T. J., and P. M. Galton. 2007. New information on the braincase and skull of *Anchisaurus polyzelus* (Lower Jurassic, Connecticut, USA: Saurischia: Sauropodomorpha): implications for sauropodomorph systematics. Special Papers in Palaeontology 77:245–260.
- Ferreira-Cardoso, S., R. Araújo, N. E. Martins, G. G. Martins, S. Walsh, R. M. S. Martins, N. Kardjilov, I. Manke, A. Hilger, and R. Castanhinha. 2017. Floccular fossa size is not a reliable proxy of ecology and behaviour in vertebrates. Scientific Reports 7:2005.
- Galton, P. M. 1984. Cranial anatomy of the prosauropod dinosaur *Plateosaurus* from the Knollenmergel (Middle Keuper, Upper Triassic) of Germany. I. Two complete skulls from Trossingen/Württ, with comments on the diet. Geologica et Palaeontologica 18:139–171.
- Galton, P. M. 1985. Cranial anatomy of the prosauropod dinosaur *Plateosaurus* from the Knollenmergel (Middle Keuper, Upper Triassic) of Germany. II. All the cranial material and details of soft-part anatomy. Geologica et Palaeontologica 19:119–159.
- Galton, P. M., and R. T. Bakker. 1985. The cranial anatomy of the prosauropod dinosaur “*Efraasia diagnostica*”, a juvenile individual of *Sellosaurus gracilis* from the Upper Triassic of Nordwürttemberg, West Germany. Stuttgarter Beiträge zur Naturkunde Serie B 117:1–15.
- Galton, P. M., and D. Kermack. 2010. The anatomy of *Pantydraco caducus*, a very basal sauropodomorph dinosaur from the Rhaetian (Upper Triassic) of South Wales, UK. Revue de Paléobiologie 29:341–404.
- Gardner, N. M., C. M. Holliday, and F. R. O’Keefe. 2010. The braincase of *Youngina capensis* (Reptilia, Diapsida): new insights from high-resolution CT scanning of the holotype. Palaeontologia Electronica 13(3):19A.
- Gower, D. J. 1997. The braincase of the early archosaurian reptile *Erythrosuchus africanus*. Journal of Zoology 242(3):557–576.
- Gower, D. J. 2002. Braincase evolution in suchian archosaurs (Reptilia: Diapsida): evidence from the rauisuchian *Batrachotomus kupferzellensis*. Zoological Journal of the Linnean Society 136:49–76.
- Gower, D. J., and E. Weber. 1998. The braincase of *Euparkeria*, and the evolutionary relationships of avialans and crocodylians. Biological Reviews 73:367–411.
- Holliday, C. M., and L. M. Witmer. 2008. Cranial kinesis in dinosaurs: intracranial joints, protractor muscles, and their significance for cranial evolution and function in diapsids. Journal of Vertebrate Paleontology 28:1073–1088.
- Janensch, W. 1935. Über Bahnen von Hirnvenen bei Saurischiern und Ornithischiern, sowie einigen anderen fossilen und rezenten Reptilien. Palaeontologische Zeitschrift 18:181–198.
- Knoll, F., L. M. Witmer, F. Ortega, R. C. Ridgely, and D. Schwarz-Wings. 2012. The braincase of the basal sauropod dinosaur *Spinophorosaurus* and 3D reconstructions of the cranial endocast and inner ear. PLoS ONE 7:e30060.
- Kurzanov, S. M. 1976. Brain-case structure in the carnosaur *Itemirus* n. gen. and some aspects of the cranial anatomy of dinosaurs. Paleontological Journal 1976:361–369.
- Langer, M. C. 2003. The pelvic and hindlimb anatomy of the stem-sauropodomorph *Saturnalia tupiniquim* (Late Triassic, Brazil). Paleobios 23:1–40.
- Langer, M. C. 2014. The origins of Dinosauria: much ado about nothing. Palaeontology 57:469–478.
- Langer, M. C., M. D. Ezcurra, O. W. M. Rauhut, M. J. Benton, F. Knoll, B. W. McPhee, F. E. Novas, D. Pol, and S. L. Brusatte. 2017. Untangling the dinosaur family tree. Nature 551:e2.
- Langer, M. C., and J. Ferigolo. 2013. The Late Triassic dinosauriform *Sacisaurus agudoensis* (Caturrita Formation; Rio Grande do Sul, Brazil): anatomy and affinities. Geological Society Special Publication 379:353–392.
- Langer, M. C., F. Abdala, M. Richter, and M. J. Benton. 1999. A sauropodomorph dinosaur from the Upper Triassic (Carman) of southern Brazil. Comptes Rendus de l’Académie des Sciences, Series IIA: Earth and Planetary Science 329:511–517.
- Langer, M. C., M. D. Ezcurra, J. S. Bittencourt, and F. E. Novas. 2010. The origin and early evolution of dinosaurs. Biological Reviews 85:55–110.
- Langer, M. C., A. M. Ribeiro, C. L. Schultz, and J. Ferigolo. 2007. The continental tetrapod-bearing Triassic of South Brazil. New Mexico Museum of Natural History and Science Bulletin 41:201–218.
- Martínez, R. N., C. Apaldetti, and D. Pol. 2012a. Basal sauropodomorphs from the Ischigualasto Formation. Journal of Vertebrate Paleontology 32(1, Supplement):51–69.
- Martínez, R. N., J. A. Haro, and C. Apaldetti. 2012b. Braincase of *Panphagia protos* (Dinosauria, Sauropodomorpha). Journal of Vertebrate Paleontology 32(1, Supplement):70–82.
- Martínez, R. N., P. C. Sereno, O. A. Alcober, C. E. Colombi, P. R. Renne, I. P. Montañez, and B. S. Currie. 2011. A basal dinosaur from the dawn of the dinosaur era in southwestern Pangaea. Science 331:206–210.
- Martz, J. W., and B. J. Small. 2006. *Tecovasuchus chatterjeei*, a new aetosaur (Archosauria: Stagonolepididae) from the Tecovas Formation (Carnian, Upper Triassic) of Texas. Journal of Vertebrate Paleontology 26:308–320.
- Müller, R. T., M. C. Langer, M. Bronzati, C. P. Pacheco, S. F. Cabreira, and S. Dias-da-Silva. 2018. Early evolution of sauropodomorphs: anatomy and phylogenetic relationships of a remarkably well preserved dinosaur from the Upper Triassic of southern Brazil. Zoological Journal of the Linnean Society 184:1187–1248. doi: 10.1093/zoolinnean/zly009.
- Nesbitt, S. J. 2011. The early evolution of archosaurs: relationships and the origin of major clades. Bulletin of the American Museum of Natural History 352:1–292.
- Nesbitt, S. J., C. A. Sidor, R. B. Irmis, K. D. Angielczyk, R. M. H. Smith, and L. A. Tsuji. 2010. Ecologically distinct dinosaurian sister groups shows early diversification of Ornithodira. Nature 464:95–98.
- Nesbitt, S. J., N. D. Smith, R. B. Irmis, A. H. Turner, A. Downs, and M. A. Norell. 2009. A complete skeleton of a Late Triassic saurischian and the early evolution of dinosaurs. Science 326:1530–1533.
- Paulina-Carabajal, A. 2012. Neuroanatomy of titanosaurid dinosaurs from the Upper Cretaceous of Patagonia, with comments on endocranial variability within Sauropoda. The Anatomical Record 295:2141–2156.
- Paulina-Carabajal, A. 2015. Guía para el estudio de la neuroanatomía de dinosaurios Saurischia, con énfasis en formas sudamericanas. Publicación Electrónica de la Asociación Paleontológica Argentina 15:108–142.
- Paulina-Carabajal, A., and P. J. Currie. 2012. New information on the braincase of *Sinraptor dongi* (Theropoda: Allosauroidea): ethmoidal region, endocranial anatomy, and pneumaticity. Vertebrata Palasiatica 4:85–101.
- Paulina-Carabajal, A., and P. J. Currie. 2017. The braincase of the theropod dinosaur *Murusraptor*: osteology, neuroanatomy and comments on the paleobiological implications of certain endocranial features. Ameghiniana 54:617–640.
- Paulina-Carabajal, A., J. L. Carballido, and P. J. Currie. 2014. Braincase, neuroanatomy, and neck posture of *Amargasaurus cazau* (Sauropoda, Dicraeosauridae) and its implications for understanding head posture in sauropods. Journal of Vertebrate Paleontology 34:870–882.
- Paulina-Carabajal, A., Y.-N. Lee, Y. Kobayashi, H.-J. Lee, and P. J. Currie. 2018. Neuroanatomy of the ankylosaurid dinosaurs *Tarchia teresae* and *Talarurus plicatospineus* from the Upper Cretaceous of Mongolia, with comments on endocranial variability among ankylosaurs. Palaeogeography, Palaeoclimatology, Palaeoecology 494:135–146.
- Piechowski, R., G. Niedźwiedzki, and M. Tałanda. 2018. Unexpected bird-like features and high intraspecific variation in the braincase of the Triassic relative of dinosaurs. Historical Biology. doi: 10.1080/08912963.2017.1418339.
- Porro, L. B., L. M. Witmer, and P. M. Barrett. 2015. Digital preparation and osteology of the skull of *Lesothosaurus diagnosticus* (Ornithischia: Dinosauria). PeerJ 3:e1494.
- Prieto-Márquez, A., and M. A. Norell. 2011. Redescription of a nearly complete skull of *Plateosaurus* (Dinosauria: Sauropodomorpha)

- from the Late Triassic of Trossingen (Germany). *American Museum Novitates* 3727:1–58.
- Rauhut, O. W. M. 2003. The interrelationships and evolution of basal theropod dinosaurs. *Special Papers in Palaeontology* 69:1–213.
- Rauhut, O. W. M. 2004. Braincase structure of the Middle Jurassic theropod dinosaur *Piatnitzkysaurus*. *Canadian Journal of Earth Sciences* 41:1109–1122.
- Rauhut, O. W. M., A. C. Milner, and S. Moore-Fay. 2010. Cranial osteology and phylogenetic position of the theropod dinosaur *Proceratosaurus bradleyi* (Woodward, 1910) from the Middle Jurassic of England. *Zoological Journal of the Linnean Society* 158:155–195.
- Sampson, S. D., and L. M. Witmer. 2007. Craniofacial anatomy of *Majungasaurus crenatissimus* (Theropoda: Abelisauridae) from the Late Cretaceous of Madagascar. *Journal of Vertebrate Paleontology* 27(2, Supplement):32–102.
- Säve-Söderbergh, G. 1947. Notes on the brain-case in *Sphenodon* and certain Lacertilia. *Zoologiska Bidrag från Uppsala* 25:489–516.
- Sereno, P. C., R. N. Martínez, and O. A. Alcober. 2012. Osteology of *Eoraptor lunensis* (Dinosauria, Sauropodomorpha). *Journal of Vertebrate Paleontology* 32(1, Supplement):83–179.
- Sobral, G., C. A. Hipsley, and J. Müller. 2012. Braincase redescription of *Dysalotosaurus lettowvorbecki* (Dinosauria, Ornithopoda) based on computed tomography. *Journal of Vertebrate Paleontology* 32:1090–1102.
- Sobral, G., R. B. Sookias, B.-A. S. Bhullar, R. Smith, R. J. Butler, and J. Müller. 2016. New information on the braincase and inner ear of *Euparkeria capensis* Broom: implications for diapsid and archosaur evolution. *Royal Society Open Science* 3:160072.
- Tykoski, R. S. 1998. The osteology of *Syntarsus kayentakatae* and its implications for ceratosaurid phylogeny. Ph.D. dissertation. University of Texas at Austin, Austin, Texas, 217 pp.
- Witmer, L. M. 1997. Craniofacial air sinus systems; pp. 151–159 in P. J. Currie and K. Padian (eds.), *Encyclopedia of Dinosaurs*. Academic Press, San Diego, California.
- Witmer, L. M., and R. C. Ridgely. 2009. New insights into the brain, braincase, and ear region of tyrannosaurs (Dinosauria, Theropoda), with implications for sensory organization and behaviour. *The Anatomical Record* 292:1266–1296.
- Yates, A. M. 2007. The first complete skull of the Triassic dinosaur *Melanorosaurus* Houghton (Sauropodomorpha: Anchisauria). *Special Papers in Palaeontology* 77:9–55.

Submitted March 2, 2018; revisions received August 30, 2018;

accepted September 16, 2018.

Handling editor: Gabriel Bever.